THE ROLE OF MACROPHAGE GLUT1-MEDIATED GLUCOSE METABOLISM IN ATHEROSCLEROSIS

Liyang Zhao

A thesis submitted to the faculty of the University of North Carolina at Chapel Hill in partial fulfillment of the requirements for the degree of Master of Science in the Department of Nutrition in the Gillings School of Global Public Health.

Chapel Hill
2015

Approved by:

Liza Makowski

Brian Bennett

Rosalind Coleman

ABSTRACT

Liyang Zhao: The Role of Macrophage GLUT1-Mediated Glucose Metabolism in Atherosclerosis
(Under the direction of Liza Makowski)

Macrophages play a key role in the pathogenesis of atherosclerosis. We recently created a novel murine model with GLUT1 specifically deleted from monocyte/macrophages. Preliminary results from our lab suggest that macrophages lacking GLUT1 reduce the pro-inflammatory response. We therefore hypothesized that macrophages with GLUT1 deletion will have reduced pro-inflammatory activation during atherogenesis, which will reduce formation of atherosclerosis in a mouse model lacking the LDL receptor (*Ldlr*$^{-/-}$). We transplanted bone marrow from *Glut1*$^{fl/fl}$ or *Glut1*$^{M\Phi-/-}$ mice into *Ldlr*$^{-/-}$ mice and fed mice a Western Diet (WD) for 12 weeks. *Glut1*$^{M\Phi-/-}$ *Ldlr*$^{-/-}$ mice exhibited significantly less plasma total cholesterol and LDL cholesterol compared to *Glut1*$^{fl/fl}$ *Ldlr*$^{-/-}$ mice. Additionally, our results demonstrated that mice with macrophages lacking GLUT1 displayed more and larger necrotic cores in atherosclerotic lesions compared to floxed transplanted controls. These results suggest that macrophage glucose metabolism mediates systemic cholesterol metabolism, and atherogenesis. Importantly, the maintenance of atherosclerotic lesion stability may be regulated by macrophage glucose metabolism-dependent mechanisms.

ACKNOWLEDGEMENTS

I would like to thank my supervisor, Dr. Liza Makowski, for her support and guidance throughout my thesis. Her patience, advice, and help were invaluable during this two yearlong study. I would also like to thank all of the members of the Makowski laboratory, past and present, for their help and support. A special thank you to Dr. Amy Johnson and Dr. Alex Freemerman for continually assist me with experiments and provide valuable input on my coursework. I would like to thank my committee members Dr. Brian Bennett for his precious advice on mouse dissection and tissues analysis; as well as Dr. Rosalind Coleman for her encouragement and career guidance. Assistance from the UNC McAllister Heart Institute was invaluable. I would also like to acknowledge Ms. Taylor Christensen's contributions to plaque analysis. Lastly, I would like to thank my friends and family for their encouragement and good humor. My thesis was supported by an award from the UNC Gillings School of Global Public Health's B. Erik and Mabel S. Johansson Scholarship, as well as a McAllister Heart Institute pilot study award to Dr. Makowski. This research was supported by grant from the American Heart Association to Dr. Makowski.

TABLE OF CONTENTS

LIST OF FIGURES

LIST OF ABBREVIATIONS

AAM	Alternatively activated macrophage
ABCA1	ATP binding cassette transporter ABCA1
ABCG1	ATP binding cassette transporter ABCG1
ACC	Acetyl CoA carboxylase
BMDMs	bone marrow derived macrophages
BMT	Bone marrow transplant
CAM	Classically activated macrophage
CD36	Cluster of differentiation 36
CETP	Cholesterol ester transfer protein
CLS	Crown like structure
ER	Endoplasmic reticulum
FAT/CD36	Long-chain fatty acyl coenzyme A
FFPE	Formalin fixed paraffin embedded
GLUT1	Glucose transporter 1
GLUT1-EV	GLUT1 empty vector
$Glut1^{M\Phi-/-}$	Macrophage specific GLUT1 knock out
$Glut1^{fl/fl}$	Floxed Glut1 gene
GLUT1-OE	GLUT1 over expresser
GSH	Reduced glutathione
GSSG	Oxidized glutathione
HFD	High fat diet
HMG-CoA	3-hydroxy—methylglutaryl coenzyme A

ICAM	Intercellular adhesion Molecule
IFN	Interferon gamma
IL-1β	Interleukin-1β
IL-6	Interleukin-6
iNOS	Inducible nitric oxide synthase
JNK	C-Jun NH_2 terminal kinase
LFA1	Lymphocyte function-associated antigen 1
LPS	Lipopolysaccharide
LXR	Liver X receptor
MCP-1	Macrophage chemotactic protein-1
M-CSF	Monocytes colony stimulating factor
MMP	Matrix metalloproteinase
NO	Nitric oxide
OCT	Optimal Cutting Temperature
ORO	Oil Red O
OxLDL	Oxidized low density lipoprotein
PAI-1	Plasminogen activator inhibitor-1
PPP	Pentose Phosphate Pathway
ROS	Reactive oxygen species
SMC	Smooth muscle cells
SR-A	Scavenger receptor class A type I/II
SREBP1	Sterol regulatory element binding protein 1
T2D	Type 2 diabetes

TNF-α	Tumor necrosis factor-α
VCAM	Vascular cells adhesion molecule
WD	Western Diet

CHAPTER I - BACKGROUND

Introduction

Atherosclerosis, affecting large and medium sized arteries, is the underlying cause of about 50% of all deaths in Westernized societies (Lusis, 2000). Factors including obesity, smoking, hypertension, elevated serum cholesterol, triglycerides, and free fatty acids, as well as decreased insulin sensitivity, are associated with increased risk of atherosclerosis. To date, there are limited relevant options to treat atherosclerosis besides prevention; therefore, further research into biological mechanisms is necessary.

Atherosclerosis is a chronic inflammatory disease characterized by four major steps including 1) initiation of endothelial activation and inflammation; 2) promotion of intimal lipoprotein deposition, retention, modification, and foam cell formation; 3) progression of complex plaques by plaque growth and enlargement of the necrotic core, fibrosis, thrombosis, and remodeling; and 4) precipitation of acute events (Hopkins, 2013).

Lesion development is initiated by deposition of cholesterol-rich and apolipoprotein B-containing lipoproteins, particularly low-density lipoprotein (LDL) in the subendothelial space of blood vessels. Physical interaction between LDL and proteoglycans causes accumulated LDL to remain in the subendothelial space. Mouse experiments show that mice expressing the proteoglycan binding– defective LDL had greatly reduced atherogenesis and that this effect was indeed due to decreased interaction of the mutated LDL with arterial wall proteoglycans (Tabas, Williams, & Boren, 2007). LDL retained within the intima can be chemically modified including

oxidation, aggregation, enzymatic or non-enzymatic cleavage, and hydrolysis all of which trigger local maladaptive responses to modified LDL (Moore, Sheedy, & Fisher, 2013). Modified LDL is pro-inflammatory, which enables it to activate overlying endothelial cells to express cell adhesion molecules such as intercellular adhesion molecule (ICAM) and vascular cell adhesion protein (VCAM) and secrete chemokines. Monocytes, attracted by activated endothelial cells are slowed down through rolling and stopped by attachment to the endothelial cells followed by transmigration to the subendothelial space. Upon stimulation by macrophage colony-stimulating factor (M-CSF) and other differentiation factors, monocytes differentiate into macrophages (Moore & Tabas, 2011). Scavenger receptor-mediated engulfment of oxidized LDL (oxLDL) transforms infiltrated macrophages to cholesterol-laden foam cells. The combination of macrophages taking up oxLDL through scavenger receptors and a lack of negative feedback keeps this engulfing process going non-stop. Eventually, accumulated cholesterol esters confer the macrophage "foam cell" characteristics. When the intracellular cholesterol content exceeds the foam cell's processing capacity, foam cells undergo apoptosis. High concentrations of cytokines such as TNFa, unesterified cholesterol or oxysterols , oxLDL, activation of the Fas death pathway by Fas ligand (32), and ER stress all promote apoptosis processes (Seimon & Tabas, 2009). Apoptotic cells are readily cleared by macrophages through phagocytosis in the early lesion, however with the progression of lesion; phagocytosis of dead cells by lesion macrophages substantially decreases. Non-cleared apoptotic cells succumb to secondary necrosis and release cellular material into the microenvironment to ultimately create the necrotic core, a hallmark of unstable atherosclerotic lesion. Lesions considered advanced by their histology may or may not narrow the arterial lumen; however such lesions may be clinically significant because complications may develop suddenly (Stary et al., 1995; Virmani, Burke, Farb, & Kolodgie,

2002). Stages of atherosclerosis are shown in Figure 1. Pathological studies suggest that the development of thrombus-mediated acute coronary events depend principally on the composition and vulnerability of a plaque rather than the severity of stenosis (Lusis, 2000). Macrophages play critical roles in promoting lesion progression through secreting pro-inflammatory cytokines, matrix degrading enzymes, and reactive oxygen species which all contribute to lesion structural disorganization. Eventually, under the stress of various detrimental factors, lesions become vulnerable, and hematoma-hemorrhage and thrombus ensue, often leading to lesion rupture, myocardial infarction, and death.

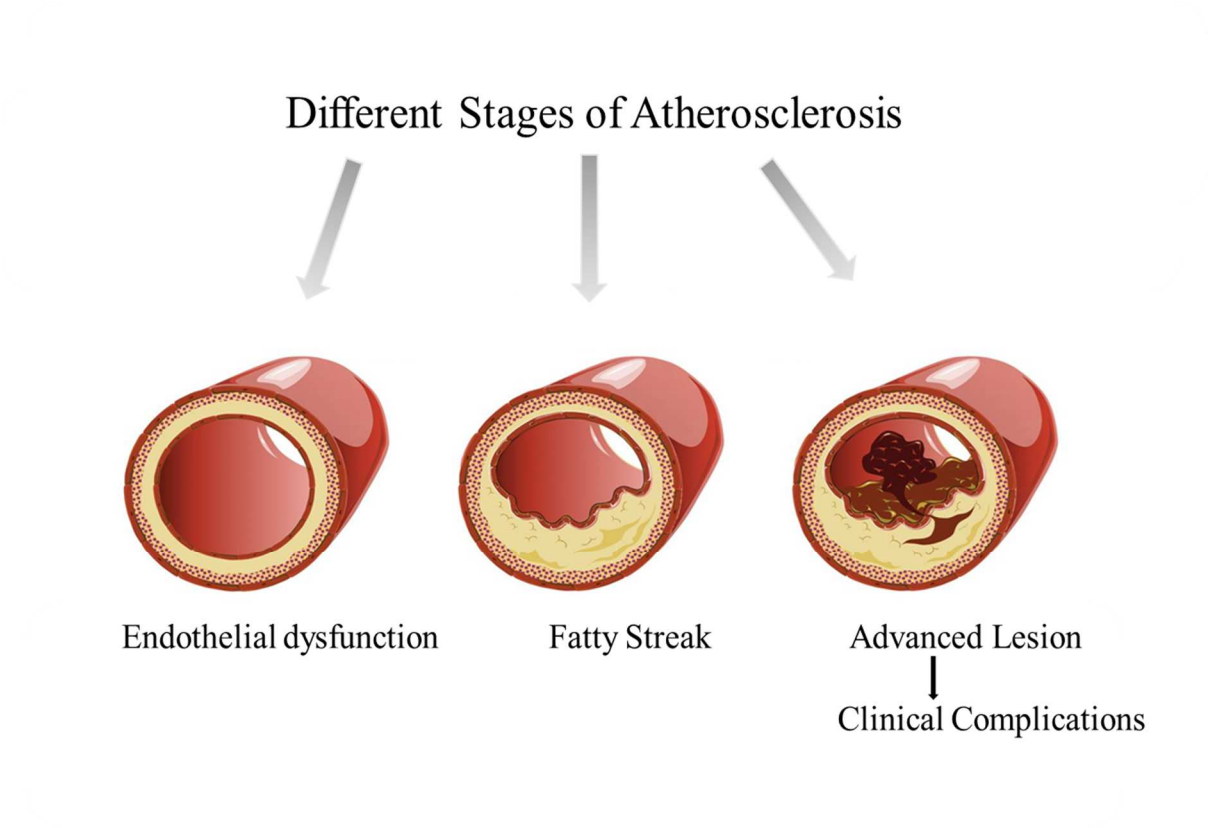

Figure 1: Illustration of the different stages of atherosclerosis (Hess, Marx, & Lehrke Michael, 2012)

Through investigating the underlying causative mechanisms promoting atherogenesis, we can find more effective prevention and treatment methods for atherosclerosis and clinical events. Atherosclerosis is a multi-factorial disease and macrophages play an unparalleled role in almost every stage of its pathogenesis. Therefore, studying macrophage biology has become a primary interest in the field. A body of evidence has demonstrated that macrophages, a critical component of the innate immune system, contribute to chronic inflammation-related pathology including obesity, insulin resistance, and atherosclerosis. Moreover, substrate metabolism is one of the mechanisms that affects the macrophage inflammatory response. Hence, the research presented herein examined the mechanistic links between macrophage substrate metabolism and the inflammatory response in atherogenesis.

Risk factors of Atherosclerosis

A large body of evidence has shown that dyslipidemia, hypertension, smoking, metabolic syndrome, diabetes, and other underling disease are atherosclerosis risk factors (Altman, 2003).

1) Dyslipidemia

Anichkov first demonstrated the role of cholesterol in the development of atherosclerosis in 1913 but the validity of the lipid hypothesis did not become generally accepted until 1984 (Steinberg, 2013). Evidence from animal studies, epidemiological studies, and clinical trials of cholesterol-lowering therapies all support that hypercholesterolemia is a salient risk factor for atherosclerosis (Fruchart, Nierman, Stroes, Kastelein, & Duriez, 2004). LDL is the major plasma cholesterol transporter and is the predominant atherogenic lipoprotein. Dietary cholesterol and cholesterol synthesized by the endogenous pathway both contribute to the total amount of cholesterol in the body. LDL is taken up by cells through LDL receptor-mediated endocytosis; the expression of LDL receptor is regulated by intracellular cholesterol concentrations. Low

intracellular cholesterol activates sterol regulatory element binding protein (SREBP) which then enters the nucleus to up-regulate LDL receptor and HMG-CoA reductase, and other enzymes in cholesterol regulation and *de novo* cholesterol synthesis pathway. Conversely, high intracellular cholesterol down-regulates LDL receptor and HMG-CoA reductase and subsequently reduces endogenous cholesterol production (Horton, Goldstein, & Brown, 2002). Uptake of plasma cholesterol through LDL receptor-mediated endocytosis not only reduces plasma cholesterol concentrations, but also signals cellular lipid synthesis machinery to stop synthesizing endogenous cholesterol. Therefore, any genetic variation or mutation affecting the process of receptor-mediated LDL endocytosis leads to elevated plasma LDL and hypercholesterolemia. Evidence indicates that high LDL promotes atherosclerosis at every stage of its pathological development. Discoveries of LDL receptor defects in familial hypercholesterolemia patients, along with clinical trials of statin drugs that decrease plasma LDL and reduce coronary morbidity and mortality, proved that LDL cholesterol is an independent risk factor of coronary heart disease (Grundy, 2002).

2) Hypertension

Hypertension is associated with increased risk of atherosclerosis and, importantly, it shares similar cellular and molecular mechanisms with atherosclerosis, particularly from the endothelium perspective. Endothelial dysfunction appears to be one of the initiators of pathogenesis for both diseases (Alexander, 1995). Removing endothelial cells facilitates atherosclerotic lesion development in animal models, indicating that functional endothelial cells protect animals from atherosclerosis. It has been demonstrated that endothelial cells overlying lesions are intact but morphologically altered. Hypertension plays a central role in promoting

endothelial cell morphology changes. Under chronic hypertensive conditions, smooth muscle cells (SMC) of blood vessels experience adaptive hypertrophy and proliferation, salient features of hypertension, which confer blood vessels greater contractility. Thickening of blood vessels by SMC hypertrophy increases the distance required for diffusion of oxygen from the lumen. This in turn results in incomplete oxidation and eventually increases free radical production, which oxidizes subendothelial-retained LDL to oxLDL. Importantly, hypertension is one of the leading causes of atherosclerotic renal disease in the US. Prehypertensive state is associated with increased presence of inflammatory markers linked to atherosclerosis and even mild hypertension serves as an important risk factor for progression of chronic kidney disease toward irreversible renal failure (Chade, Lerman, & Lerman, 2005). The pathogenesis of hypertension, like atherosclerosis, is extremely complicated. More importantly, it can enhance atherosclerosis through various other processes and remains one of the most relevant independent risk factors of atherosclerosis (Alexander, 1995).

3) Diabetes

Patients with type 2 diabetes (T2D) have an increased risk of cardiovascular morbidity and mortality. T2D and atherosclerotic vascular disease have shared pathogenic pathways, in which insulin resistance and abdominal obesity play central roles (Wassink et al., 2008). Macrophages, as an important component of the innate immune system, have been discovered to be the common culprit for both the pathogenesis of abdominal obesity related and insulin resistance (Chawla, Nguyen, & Goh, 2011). In obesity-induced insulin resistance, macrophages polarize to pro-inflammatory phenotypes and secrete cytokines, including interleukin-1β (IL-1 β), tumor necrosis factor-α (TNF-α), interleulink-12 (IL-12), *etc*. Pro-inflammatory cytokines, notably

TNF-α, disrupt insulin signaling pathways by phosphorylating insulin receptor substrate 1 (IRS1) 307 serine and result in insulin resistance and eventually T2D. Furthermore, insulin resistance and T2D lead to hypercholesterolemia through increased lipolysis and decreased lipid clearance. Through sharing the same pathogenesis and directly causing dyslipidemia, T2D accelerates atherosclerosis.

4) Other risk factors

Atherosclerosis is a multifactorial disease: both genetic and environmental factors promote its development. Recent studies have characterized monocytosis, which is defined as elevated monocyte numbers in the circulation, as another independent risk factor for coronary artery disease in humans (Randolph, 2014). Studies have shown that hypercholesterolemia is associated with monocytosis through promotion of hematopoietic cell proliferation, signaled by alteration of cholesterol levels on hematopoietic stem cells, in mice, pigs, and rabbits (Moore et al., 2013; Randolph, 2014). Moreover, recent compelling evidence has shown that ApoE is able to regulate monocyte pool size (Randolph, 2014), demonstrated by the fact that *ApoE*$^{-/-}$ mice show a 50% increase in monocyte numbers relative to wild type mice (Moore et al., 2013). Interestingly, in hypercholesterolemic mice, monocytosis is mainly derived from an increase in the more inflammatory LY6C^{hi} subset (Moore et al., 2013).

Mouse Models of Atherosclerosis

Due to the inexpensive cost, easy genetic manipulation, and relative short time frame of atherosclerosis development, murine models have been extensively used in atherosclerosis research (Getz & Reardon, 2012). Despite being the most favored species for atherosclerosis investigation, differences exist between mice and humans regarding lipid metabolism, risk factors, and pathological processes of atherosclerosis. For example, unlike humans, HDL is the

major lipoprotein in mice, and subsets of HDL in mice differ from human. Both of these characteristics render mice resistant to atherogenesis (Getz & Reardon, 2012). Murine models including mutations of LDL receptors or ApoE that increase LDL cholesterol, have distinct features: 1) most mouse models do not develop unstable atherosclerotic plaques, whereas in humans, a vulnerable plaque is the leading cause for a clinical acute cardiovascular event; 2) mouse models do not form thick fibrous caps which are frequently seen in human chronic atherosclerotic plaques; 3) mouse models develop the majority of plaques in the aortic root, but rarely in coronary artery, unlike humans; 4) in the mouse peripheral blood, there are approximately 50% pro-inflammatory monocytes ($LY6C^{hi}$) and 50% anti-inflammatory monocytes ($LY6C^{low}$) circulating; whereas in humans the ratio of pro-inflammatory to anti-inflammatory monocytes is approximately 9:1 (Moore et al., 2013; Randolph, 2014). Although differences in the characteristics of atherosclerosis exist between men and mice, murine models undeniably have contributed tremendously to our understanding of the mechanisms of atherogenesis (Getz & Reardon, 2012). Due to LDL receptor and ApoE's critical functions in plasma lipoprotein levels, *Apoe*$^{-/-}$ and *Ldlr*$^{-/-}$ mouse models are two of the most frequently used mouse models for atherosclerosis research (Getz & Reardon, 2012).

ApoE knockout mice were developed in 1992 by Dr. Maeda Nobuyo's group at University of North Carolina at Chapel Hill, NC. ApoE serves as the ligand to mediate the uptake of chylomicrons, VLDL, and their remnants by hepatocyte LDL receptor and LDL receptor-related protein (Kolovou, Anagnostopoulou, Mikhailidis, & Cokkinos, 2008). Due to lack of ApoE in lipoprotein, *Apoe*$^{-/-}$ mice have reduced ability to clear plasma lipoprotein and therefore develop pronounced hypercholesterolemia, hypertriglyceridemia, and spontaneous atherosclerosis. *Apoe*$^{-/-}$ mice develop spontaneous fatty streaks in the proximal aorta at 3 months

of age and aortic sinus plaques at 8 months of age. When exposed to an atherogenic diet, *Apoe*$^{-/-}$ mice develop abundant and large aortic plaques after 14 weeks of diet exposure. ApoE is expressed in bone marrow-derived cells, mostly in the monocyte/macrophage lineage. Transfer of bone marrow cells from *ApoE*$^{-/-}$ mice into wild type mice increases aortic root atherogenesis independent of effects on plasma lipid concentration; therefore, macrophage-derived ApoE plays a large role in this model of atherosclerosis (Getz & Reardon, 2012).

The *Ldlr*$^{-/-}$ mouse model was developed by Dr. Joachim Herz one year after the successful development of *ApoE*$^{-/-}$ mice. Previous studies have demonstrated that *Ldlr*$^{-/-}$ mice display moderate increases plasma lipids and develop no or only mild atherosclerosis when fed a regular chow diet. The Paigen diet (1.25% cholesterol, 7.5% cocoa butter, 7.5% casein, and 0.5% sodium cholate) and Western Diet (21% fat and 0.15% to 0.25% cholesterol) are the most widely used high-fat regimens to accelerate atherosclerosis in the *Ldlr*$^{-/-}$ mouse. When exposed to Western Diet (WD), *Ldlr*$^{-/-}$ mice show the presence of advanced lesions in the aortic sinus after 3 months and in the innominate artery at 6 to 9 months on diet (Ma et al., 2012). Anatomy of aorta is shown in Figure 2.

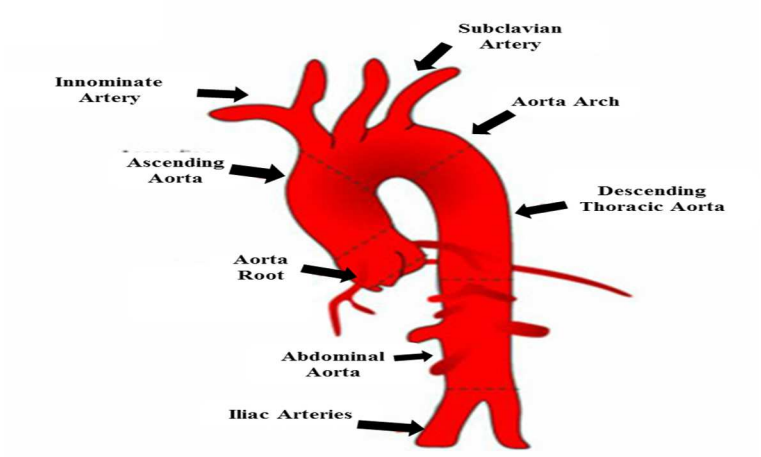

Figure 2: Aorta anatomy (Di Luozzo, 2012).

Bone marrow transplant (BMT) serves as an extremely powerful tool for atherosclerosis studies. Transplanting bone marrow cells into atherogenic mouse models is useful in studying the roles of hematopoietic cells on atherosclerosis (Getz & Reardon, 2012). To accomplish BMT, atherogenic mice receive a lethal dose of irradiation prior to receiving bone marrow from either wild type mice or genetically modified mice. After reconstitution, chimeric atherogenic mice carry transplanted hematopoietic stem cells, allowing for the study of specific roles from newly transplanted blood cells. While BMT is a powerful tool to study the contribution of hematopoietic cells, some disadvantages include that irradiation in the recipient may not ablate 100% of the hematopoietic system, irradiated mice do not gain as much weight on high fat diets (HFD) after irradiation, and, finally, irradiation can cause permanent damage to various tissues.

Roles of Macrophages in Atherosclerosis

Macrophages, central effectors of innate immunity, are recognized as key pathophysiologic agents in wide-spread disease processes associated with chronic inflammation and aging, including cancer, obesity-induced insulin resistance, and atherosclerosis (Moore & Tabas, 2011). Macrophages play a central role in the pathogenesis of atherosclerosis and investigating macrophage function has become a fundamental interest in understanding initiation, progression, and regression of atherosclerosis (Dickhout, Basseri, & Austin, 2008).

The roles of macrophages in atherosclerosis are diverse, including: 1) being the precursors of foam cells; 2) secreting pro-inflammatory cytokines, chemokines, reactive oxygen species (ROS), reactive nitrogen species (RNS), matrix degrading enzyme, and anti-inflammatory cytokines; 3) and contributing primarily to unstable plaque through imbalanced apoptosis and efferocytosis (Moore et al., 2013). Macrophages sequester cholesterol within the atherosclerotic plaque and, more importantly, are implicated in critical events such as plaque

rupture (Randolph, 2014). During the initiation stage of atherosclerosis, through continual uptake of oxidized apolipoprotein B containing lipoproteins by scavenger receptor type A (SR-A) and CD36, macrophages clear sequestered lipoproteins in the subendothelial space. This is at first beneficial in restricting lesion expansion. However, there is little negative feedback following lipid uptake, and macrophages continually engulf lipoproteins and ultimately become cholesterol-laden foam cells (Moore et al., 2013). Unregulated lipid accumulation in macrophages results in increased secretion of pro-inflammatory cytokines, accelerated apoptosis and necrosis, defective phagocytic capacities, and reduced cell migration. All dysregulated macrophage functions lead to progression of atherosclerosis and finally cause "complex" atherosclerotic lesion formation. During the progression of atherosclerosis, macrophage inflammatory responses accelerate changes in lesion morphology, notably necrotic core formation and thinning of the fibrous cap, which are characteristic of the "vulnerable" lesions that most often lead to severe cardiac events and death (Moore & Tabas, 2011). Combined effects of increased macrophage apoptosis and defective macrophage clearance result in necrotic core formation. Besides pro-inflammatory cytokines, foam cells also secrete matrix metalloproteinases which degrade collagen, elastin, and proteoglycans in the extracellular matrix, thus promoting thinning of the fibrous cap. Macrophages orchestrate the aforementioned activities, highlighting their essential contributions to the underlying mechanism(s) for the progression and aggravation of atherosclerosis. There are many steps in the process by which macrophages contribute to atherogenesis.

1) Monocyte recruitment: traffic into lesions

Atherosclerotic lesions tend to be distributed at the inner curvatures and branch points of arteries. These are target sites for macrophage deposits due to increased endothelial cell

activation. Turbulent flow, hypertension, or other pro-atherogenic factors, such as oxLDL, activate endothelial cells. Upon activation, endothelial cells express chemokines that attract monocytes expressing cognate chemokine receptors. Activated endothelial cells subsequently express selectins and cell adhesion molecules, specifically ICAM and ACAM, which recognize respectively monocyte cell surface selectin ligands and cell adhesion molecules receptor integrins. Finally, firm adhesion of monocytes is followed by their entry into the subendothelial space (a process called diapedesis) (Moore & Tabas, 2011).

Since the discovery of distinct subsets of monocytes in peripheral circulation systems by Geissmann in 2003 (Geissmann, Jung, & Littman, 2003), monocyte subsets have become an extensively investigated topic. In Both human and mouse monocytes fall into at least 2 phenotypically distinct subsets: $LY6C^{hi}$ (which are also phenotypically $Gr\text{-}1^{+}CCR2^{+}CX3CR1^{lo}$) and $LY6C^{loW}$ (which are also phenotypically $Gr\text{-}1^{-}CCR2^{-}CX3CR1^{hi}$) mouse monocytes correspond to human $CD14^{hi}CD16^{-}$ and $CD14^{+}CD16^{+}$ monocytes (Swirski et al., 2007). In mice, hypercholesterolemia is associated with an increase in the pro-inflammatory $LY6C^{hi}$ monocyte subset which participates in the acute response to inflammation. $LY6C^{low}$ monocytes are implicated in inflammation resolution. $LY6C^{hi}$ monocytes more readily enter atherosclerotic lesions than anti-inflammatory $LY6C^{low}$ monocytes. $LY6C^{low}$ cells express fewer integrin molecule LFA1 than $LY6C^{high}$ (Moore & Tabas, 2011; Moore et al., 2013). Importantly, in mice there are almost similar quantities of $LY6C^{hi}$ and $LY6C^{low}$ monocytes in circulation; in contrast, 95% of circulating monocytes in humans possess $LY6C^{hi}$, which may account for why humans are more prone to develop atherosclerosis than mice.

2) Macrophage becomes foam cells:

Modified LDL is able to activate endothelial cells, and endothelial activation in turn attracts more apoB-containing lipoproteins entering atherosclerotic lesion and retains them there. Accumulated LDL is modified by oxidation, acetylation, and aggregation. Upon arrival, macrophages starts engulfing modified LDL that are recognized by several macrophage pattern recognition receptor including SR-A1, CD36, SR-A2, CD68, SR-B1, and LOX-1. The majority of cholesterol in LDL exists in the form of cholesterol ester which, after internalization by the macrophage, is hydrolyzed to free cholesterol and fatty acids in late endo-lysosome, while free cholesterol undergoes re-esterification by ACAT to cholesterol ester. Cholesterol ester is stored in membrane-bound lipid droplets, therefore remains as a relatively inert form which confers foam cells "foam" characteristics (Moore et al., 2013). Unesterified or "free" cholesterol traffic from lysosomes to the plasma membrane and thus may become available for efflux out of the cell. However, free cholesterol has cytotoxic effects on cells, accumulation of which causes cell apoptosis or even necrosis (Moore & Tabas, 2011). SR-A1 and CD36 are among the most studied macrophage scavenger receptors. *In vivo* experiments demonstrate that deleting either SR-A1 or CD36 significantly reduces atherosclerosis in *ApoE*$^{-/-}$ mice, clearly demonstrating that uptake of oxLDL by macrophages is critical in promoting atherogenesis (Boullier et al., 2001). Phospholipid constitutes the largest majority of lipid on the surface of LDL while neutral lipids are mainly located in lipid core. Evidence suggests that oxidized phospholipid is the most relevant component in mediating binding between scavenger receptors and oxLDL. Physiologically, macrophage scavenger receptors recognize apoptotic cells and bacteria, and eventually contribute to clearance of dead cells and infection, the process of which maintains homeostasis of organisms. It was speculated that oxLDL share similar surface modules, such as

oxidized phospholipids, with apoptotic and bacterial cell membranes and are therefore taken up as foreign bodies. Although the uptake of oxLDL by scavenger receptors could cause detrimental effects for cardiovascular systems, the role of scavenger receptors in innate immunity have persisted due to natural selection (Boullier et al., 2001).

3) Foam cell inflammation

Cholesterol uptake or accumulation drives macrophage activation through direct or indirect mechanisms. Directly, oxLDL acts as a ligand for pattern recognition receptors such as scavenger receptors and toll like receptors (TLRs). Depending on the extent of oxidation, oxLDL serves as agonist of either CD14-TLR4-MD2 or CD36-TLR4-TLR6 immune receptor complexes to activate a pro-inflammatory signal cascade which involves IL-1 receptor-associated kinase 4 (IRAK4), myeloid differentiation primary-response protein 88 (MYD88), and NF- κB. Activation of NF-κB induces target gene expression including pro-inflammatory cytokines IL-1, IL-6, IL-12, IL-23, TNFα, and macrophage chemotactic protein-1 (MCP-1), which may all contribute to atherogenesis (Peled & Fisher, 2014). Furthermore, accumulated free cholesterol in cell membrane lipid rafts can activate TLR signaling pathway as well, which further magnifies NF-κB activation and targeted cytokine production. Cholesterol also induces the macrophage pro-inflammatory response indirectly by activating the NOD-like receptor family, pyrin domain containing 3 (NLRP3) Inflammasome pathway. Cholesterol crystals are present in early diet-induced atherosclerotic lesions and their appearance coincides with first appearance of inflammatory cells (Duewell et al., 2010). Both engulfed or *de novo* synthesized cholesterol crystals activate the NLRP3 Inflammasome which leads to the secretion of pro-inflammatory cytokines IL-1β and IL-18 (Peled & Fisher, 2014).

Besides activating a pro-inflammation pathway, cholesterol loading in macrophages affects cells in various other aspects. Proteins involved with cytoskeletal regulation, vesicle-mediated transport, lipid binding, and apolipoprotein E are among the proteins most upregulated in peritoneal macrophages obtained from chow- *vs*. WD fed *Ldlr*−/− mice (Becker et al., 2010; Moore & Tabas, 2011). Boyle et al. demonstrated that TNFα secreted by macrophages together with Fas ligand (FasL) on macrophage cell membrane contributes to the vascular SMC apoptosis (Boyle, Weissberg, & Bennett, 2003). SMC is the only cell type that synthesizes extracellular collagens in an atherosclerotic lesion. Decreased collagen synthesis through impairing SMC function or reducing SMC numbers, and increased collagen degradation mediated by macrophage derived matrix metalloproteinases (MMP) result in thinning of the fibrous cap, which leads to "vulnerable lesion" formation. Alternatively activated macrophages (AAM) secrete TGFβ which is an important inducer for SMC collagen biosynthesis; however, TGFβ secretion is reduced in complex lesions, which substantially decreases SMC collagen synthesis and increases the vulnerability of these lesions (Moore & Tabas, 2011).

4) Foam cell apoptosis and secondary necrosis

Mechanisms promoting foam cell apoptosis include existence of extracellular oxLDL, accumulation of high concentrations of intracellular free cholesterol, production of pro-apoptotic cytokines such as TNF-α, excessive ROS production, growth factor withdrawal, hypoxia and direct cell–cell interactions such as binding of Fas-ligand to Fas (Schrijvers, De Meyer, Herman, & Martinet, 2007). Death of macrophages elicits complicated consequences regarding atherosclerosis outcome (Van Vre, Ait-Oufella, Tedgui, & Mallat, 2012). In the early stages of atherosclerosis, apoptotic foam cells are effectively cleared by phagocytes, therefore increased foam cell apoptosis is beneficial in terms of inhibiting plaque progression. However, in the

absence of clearance, apoptotic cells rapidly expose phosphatidylserine on the surface, which is a potent activator in the generation of thrombin and activation of the coagulation cascade; simultaneously, apoptotic cells progress to secondary necrosis and autolyse, releasing potentially dangerous cellular components (Schrijvers et al., 2007). With the progression of atherosclerosis, a majority of subendothelial macrophages become cholesterol-laden foam cells and gradually demonstrate less phagocytic capacity; hence, macrophage apoptotic cells and extracellular lipid accumulate in lesion plaques, form the necrotic core which is the hallmark of an unstable plaque and ultimately may lead to cardiovascular events through rupture of the lesion.

5) Efferocytosis

Macrophage apoptosis by itself will not trigger plaque necrosis. Rather, plaque necrosis results when apoptotic macrophages are not sufficiently cleared by phagocytes (efferocytosis) (Moore & Tabas, 2011). If apoptotic foam cells are not cleared efficiently by phagocytes, they eventually undergo a secondary necrosis process and subsequently release toxic intracellular contents including large amounts of tissue factors which trigger the coagulation cascade and thrombosis formation. Therefore, effective removal of apoptotic cell debris prevents unstable plaque development, whereas, reduced phagocytosis of apoptotic cells increases vulnerability of the atherosclerotic plaque. Furthermore, efferocytosis activates phagocytes to express IL-10 and TGFβ which mount an anti-inflammatory response, and it promotes survival of the efferocytes themselves so that they do not succumb to potentially toxic factors in apoptotic cells (Moore & Tabas, 2011). Professional phagocytes, such as macrophages and dendritic cells, rapidly recognize an apoptotic cell surface's "eat me" signals, such as phosphatidylserine, and eventually phagocytize apoptotic cells (Schrijvers et al., 2007). Phagocytosis, which is the uptake of large particles (>0.5μm), involves active actin cytoskeleton rearrangement and remodeling. It is

known that efferocytosis in atherosclerotic lesions is defective, however the underlying mechanisms are poorly studied. Venter et al. recently demonstrated that the capacity to undergo LPS-induced cell shape changes and to phagocytize particles does not depend on oxidative phosphorylation activity but is fueled by glycolysis. They postulated that in macrophages, glucose critically participates in non-metabolic regulation of actin cytoskeletal remodeling via posttranslational modification of receptors or signaling molecules (Venter et al., 2014). Other evidence suggests that effective phagocytosis requires macrophages to have intact lipid metabolism to maintain effective cholesterol esterification and efflux (Moore et al., 2013). Hence, while the role of metabolism in macrophage-mediated phagocytosis has been demonstrated, the exact substrates and metabolic pathways remain unclear. Illustration of the role of apoptosis and efferocytosis on atherosclerosis is shown in Figure 3.

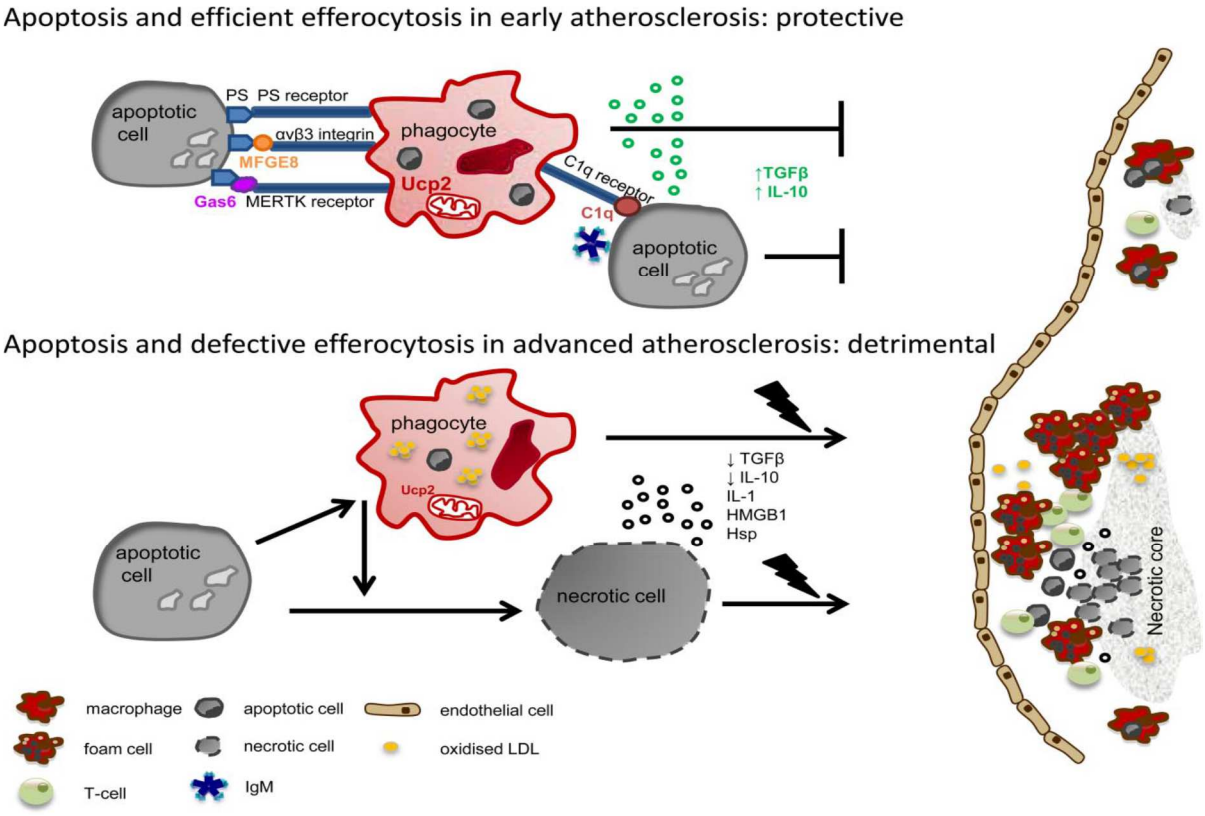

Figure 3. The role of efferocytosis and apoptosis on atherosclerosis (Van Vre et al., 2012).

6) **Macrophage egress and lipid efflux**

It has been shown that macrophages can emigrate out of atherosclerotic lesions, and this phenomena happens more in the early stage of atherosclerosis. Moore et al. demonstrated that both cholesterol loading and hypoxia increase the expression of the neuro-immune guidance cues Netrin-1 and Semaphorin-3E which are encoded by gene *Ntn-1* and *Sema3e* in mice , both of which function to induce macrophage chemostasis *in vitro*. Chimeric $Ldlr^{-/-}$ mice carrying deficient macrophage netrin1 display reduced atherosclerosis progression and increased macrophage emigration from lesions, suggesting that Netrin-1 may function to retain macrophages in plaques (Moore et al., 2013). Cells sense increased intracellular cholesterol content and decrease endogenous cholesterol synthesis and LDL receptor expression regulated by SREPB1, and increase expression of ATP binding cassette transporter A1 (ABCA1) and ATP binding cassette transporter G1 (ABCG1) through activation of LXR by cholesterol derivatives oxysterols and desmosterol. ABCA1 and ABCG1 are members of ATP-binding cassette superfamily participating in cholesterol efflux. Specifically, ABCA1 transfers cholesterol to lipid-poor APOA1 of HDL, and ABCG1 pumps cholesterol to mature HDL particles (Moore et al., 2013). This is a process called reverse cholesterol transport and understanding the role of macrophages in removal of cholesterol from plaques is vital.

7) Macrophage polarization and inflammatory response

In response to different metabolic and immune stimuli of the microenvironment, macrophages display a spectrum of phenotypes (Odegaard et al., 2007a). Relative to total numbers of macrophages, their subsets might be a better indicator of plaque phenotypes and stability. Based on cell surface expression markers, production of cytokines, and their biological function, macrophages are categorized into several classes (Chinetti-Gbaguidi, Colin, & Staels,

2015), notably classically activated macrophages (CAM), alternatively activated macrophages (AAM), and a spectrum of intermediate classes. Macrophages are activated by infection, cytokines such as IFNγ, or saturated fatty acids through classical activation pathway. Upon activation, CAMs secrete high concentrations of TNFα, IL-1β, IL-12, and IL-23, but low levels of IL-10 and TGFβ. *INFγ*$^{-/-}$ */apoE*$^{-/-}$ double knock-out mice display significantly smaller atherosclerotic lesion than *ApoE*$^{-/-}$ mice, and exhibit a substantial increase in their collagen content, which indicate that loss of Th1 signaling polarizes macrophages to the less-inflammatory state (Vats et al., 2006). From a functional point of view, CAMs participate in the removal of pathogens during infection through activation of the NADPH oxidase system and production of pro-inflammatory cytokines. In contrast, AAMs stimulated by type 2 T-helper cytokines IL-4 or IL-13 express IL10, IL-1 receptor antagonist, arginase-1, transforming growth factor; therefore, they are implicated in tissue remodeling and wound repair and categorized as anti-inflammatory. Functionally, AAMs can scavenge debris and apoptotic cells and promote plaque fibrosis (Chinetti-Gbaguidi et al., 2015; Johnson, Milner, & Makowski, 2012). In addition to the CAM and AAM subpopulations, other specific and distinct macrophage phenotypes exist in the heterogeneous and complex environment of the atherosclerotic plaque. Macrophages are extraordinarily plastic and can switch from one phenotype to another depending on the environmental cues (Chinetti-Gbaguidi et al., 2015). Due to their plasticity and apparent contrasting roles in innate immune systems, manipulation of macrophage populations can mitigate or exacerbate disease pathology (Johnson et al., 2012), for instance, in atherosclerosis, plaque composition influences the phenotype of macrophages, while macrophage subtypes in turn affect plaque structure and evolution resulting from their intrinsic activities (such as phagocytosis) and ability to release pro-inflammatory and anti-inflammatory factors (Chinetti-

Gbaguidi et al., 2015). Thus, the composition of CAM to AAM ratios in the microenvironment of the vessel and plaque are very important.

8) The Role of macrophage substrate metabolism in their inflammatory response

Metabolism and immunity are two fundamental systems of metazoans. The presence of immune cells such as macrophage in metabolic tissues suggests a dynamic and on-going crosstalk between these two regulatory systems (Chawla et al., 2011). In 2003, Xu et al. and Weisberg et al. demonstrated that macrophage infiltration caused elevated expression of pro-inflammatory cytokines in adipose tissue of obese mice. TNFα, a cytokine largely produced by CAMs, promotes insulin resistance through phosphorylating serine 307 of insulin receptor substrate 1 (IRS1) - further demonstrating that macrophages play a critical role in metabolic disease (Chawla et al., 2011). Vats et al. demonstrated that in response to IL-4, signal transducer and activator of transcription 6 (STAT6) and PPARγ coactivator-1β (PGC-1β) induce macrophage metabolic programs for fatty acid oxidation and mitochondrial biogenesis. Increased glucose uptake and suppressed fatty acid uptake in CAMs, increased fatty acid uptake and elevated β-oxidation in AAMs indicated for the first time that there is a switch in nutrient utilization when macrophage shift from CAMs to AAMs (Vats et al., 2006). Etomoxir, mitochondrial inhibitor of fatty acid metabolism completely abolished macrophages' anti-inflammatory effects stimulated by IL-4. In contrast, inhibition of mitochondrial respiration did not have effect on inflammatory activation of macrophages stimulated by INFγ and lipopolysaccharide (LPS). Importantly, the aforementioned effects are independent of signal transducer and activator of Transcription 6 (STAT6) or peroxisome proliferator-activated receptor γ coactivator 1β (PGC-1β), suggesting direct involvement of mitochondrial oxidative metabolism in full expression of the anti-inflammatory AAM phenotype (Vats et al., 2006).

From a functional point of view, macrophage metabolic pathways that are either dependent upon glycolysis or oxidative phosphorylation, are critical for maintaining proper host defense. Glycolysis rapidly provides ATPs which are required by the respiratory burst to produce reactive oxygen species (ROS) and reactive nitrogen species (RNS) by CAMs to combat acute bacterial infection. In contrast, fatty acid oxidation provides a long-term energy supply which is needed by AAMs to secrete or express TGFβ, IL-10, and arginase I to fight intracellular parasite infections (Vats et al., 2006).

Glucose Transporter 1 and its function on Macrophage

Glucose transporter (GLUT) family and the sodium-dependent glucose transporter (SGLT) family are two classes of hexose transporters moving glucose into the cells. The GLUT family includes fourteen hexose transporters (twelve in mouse) which are facilitative transporters that transport sugars along the concentration gradient. The most widely expressed hexose transporter is GLUT1 which is thought to maintain basal glucose transport in most types of cells (Young et al., 2011). Glucose is a critical component in the pro-inflammatory response of macrophages. Previous work from our group demonstrated that GLUT1 is the primary rate limiting glucose transporter on pro-inflammatory CAMs. Furthermore, in HFD-fed rodents, macrophages in crown-like structures and inflammatory loci in adipose and liver, respectively, stain positively for GLUT1. Freemerman et al. stably over-expressed the GLUT1 transporter in RAW264.7 macrophages (GLUT1-OE). Gene expression and proteome profiling analysis revealed that GLUT1-OE macrophages developed a hyper-inflammatory state characterized by elevated secretion of inflammatory mediators. Finally, ROS production and evidence of oxidative stress were significantly enhanced in GLUT1-OE macrophages. Importantly, inhibition of glycolysis using 2-deoxyglucose as well as antioxidant treatment blunted the expression of

inflammatory mediators such as PAI-1, suggesting that glucose-mediated metabolism and oxidative stress were driving the pro-inflammatory response in a GLUT1-dependent manner. These results indicated that increased utilization of glucose, induced a ROS-driven pro-inflammatory phenotype in macrophages. Based on the *in vitro* overexpression data, the Makowski lab created a novel macrophage GLUT1-deficient mouse model to determine the contribution of GLUT1-mediated glucose metabolism to *in vivo* metabolic dysfunction. Recent work suggests that lack of GLUT1 reduced the pro-inflammatory response and the ability for GLUT1$^{-/-}$ macrophages to polarize to the classically activated state *in vitro*, which may play an integral role in the promotion of obesity-associated insulin resistance or atherogenesis.

Rationale and Hypotheses

Our previous work indicates that when macrophage fuel substrates are modulated *in vitro* simply by increasing uptake of glucose through overexpression of GLUT1 in RAW 264.7 cells, the response is dramatically driven toward pro-inflammatory or CAM-like phenotype. In order to investigate the effects of macrophage glucose metabolism *in vivo*, the Makowski lab created a novel mouse model wherein GLUT1 is specifically deleted in the monocyte/macrophage lineage through crossing a *LysM-Cre* mouse and *Glut1$^{fl/fl}$* mice to generate *Glut1$^{MΦfl/fl}$ or Glut1$^{MΦ-/-}$ mice*. Studies demonstrated that abolishing glucose metabolism in bone marrow derived macrophages from *Glut1$^{MΦ-/-}$* mice substantially decreased their capacity to mount a pro-inflammatory CAM response (manuscript in preparation). Interestingly, to test systemic effects of reduced glucose metabolism in macrophages in diet-induced obesity, mice were fed HFD or low fat diet from weaning and sacrificed at 24 weeks of age. There were slight but not significant increases in body weight in *Glut1*$^{MΦ-/-}$ compared to controls. In spite of the reduced inflammatory response in bone marrow derived macrophages (BMDMs), we observed more macrophage infiltration in

white adipose tissue from *Glut1*$^{MΦ-/-}$ mice compared to *Glut1*$^{fl/fl}$ controls. However, the macrophages in *Glut1*$^{MΦ-/-}$ were shifted towards AAM-polarized, not CAM-polarized as would be expected in obesity. Therefore, it appears that the lack of GLUT1-mediated glucose metabolism in macrophages blocked CAM-polarization and release of pro-inflammatory cytokines, even in an obese state.

The objective of this proposal is to ask if reduced macrophage glucose metabolism will also halt the formation of atherogenesis using the *Ldlr*$^{-/-}$ atherosclerosis mouse model. **We hypothesize that macrophages with blunted glucose metabolism due to lack of GLUT1 will have limited inflammatory activation during atherogenesis and reduced plaque burden**. In order to investigate the effect of deletion of macrophage GLUT1 on the pathogenesis of atherosclerosis, we transplanted bone marrow from *Glut1*$^{fl/fl}$ and *Glut1*$^{MΦ-/-}$ into the *Ldlr*$^{-/-}$ model. After 12 weeks WD feeding, we assessed atherosclerosis lesion formation status. The results are expressed in Chapter 2.

CHAPTER II - MANUSCRIPT

Macrophages play a key role in the pathogenesis of atherosclerosis. Metabolic programs powered by glucose or lipids enable macrophages to elicit pro- or anti-inflammatory responses, respectively. Although the chronic inflammatory feature of atherosclerosis has been well-established, the role of macrophage substrate metabolism in atherogenesis remains unclear. We previously demonstrated that macrophages with elevated GLUT1-mediated glucose metabolism have an increased inflammatory response. Therefore, we created a novel macrophage GLUT1-deficient murine model by crossing floxed GLUT1 mice to LysM-Cre mice. Pilot studies suggest that lack of GLUT1 reduces the pro-inflammatory response and the ability for *Glut1*$^{-/-}$ macrophages to polarize to the classically activated state *in vivo*. Therefore, the objective of this study was to examine how macrophage metabolic reprogramming affects the development of atherosclerosis. We hypothesized that macrophages with restricted glucose metabolism due to lack of glucose transporter GLUT1 will have reduced pro-inflammatory activation during atherogenesis. We transplanted bone marrow from *Glut1*$^{fl/fl}$ or *Glut1*$^{M\Phi-/-}$ mice into *Ldlr*$^{-/-}$ mice and fed mice a WD for 12 weeks. *Glut1*$^{fl/fl}$ *Ldlr*$^{-/-}$ or *Glut1*$^{M\Phi-/-}$ *Ldlr*$^{-/-}$ chimeric mice did not exhibit significant differences in body weight, body composition, blood pressure, fasting blood glucose, or triacylglycerol and HDL cholesterol concentrations. However, *Glut1*$^{M\Phi-/-}$ *Ldlr*$^{-/-}$ mice had significantly less plasma total cholesterol and LDL cholesterol compared to *Glut1*$^{fl/fl}$ *Ldlr*$^{-/-}$ mice. Digital histology analysis of Oil Red O (ORO) stained slides indicated that deletion of macrophage *Glut1* did not affect total lesion area in aortic root; however, mice with blunted glucose metabolism displayed more and larger necrotic cores. In summary, we observed that

mice lacking macrophage GLUT1 had higher plasma cholesterol and developed increased necrotic cores in lesions of the aorta root relative to mice with wild type macrophage GLUT1, suggesting that macrophage glucose metabolism mediates systemic cholesterol metabolism; and, importantly, maintenance of atherosclerotic lesion stability may be regulated by macrophage-specific glucose-dependent mechanisms.

Introduction

Atherosclerosis, a major cause of cardiovascular disease (CVD), is chronic inflammation that can proceed to acute clinical events by thrombosis and plaque rupture (Frostegard, 2013; Lusis, 2000). Atherosclerosis is tied to many risk factors including obesity, smoking, hypertension, elevated serum cholesterol, triglycerides, and free fatty acids, as well as decreased insulin sensitivity. Similar to obesity, one important driving force of atherogenesis is a microenvironment of chronic inflammation. Macrophage infiltration, partially due to overexpression of either MCP1 or its receptor CCL2, is implicated in local inflammation and insulin resistance (Odegaard et al., 2007a). There has been substantial progress in understanding the role of macrophages contributing to inflammation of vessels and adipose; however, the role of metabolism in regulating inflammation in atherosclerosis is poorly understood. Macrophages are involved in almost every stage of atherosclerosis, including but not limited to: 1) in the early stages: macrophages become foam cells through unabated engulfment of lipids, clearing neighboring dead cells, and secreting a spectrum of pro-inflammatory cytokines; 2) in the advanced stages: macrophages release matrix degrading enzymes, pro-coagulant tissue factors, and promote SMCs death. The integration of inflammation and lipid signaling in macrophages contributes significantly to the pathogenesis of atherosclerosis, insulin resistance, and obesity through multiple pathways. These pathways include the nuclear hormone receptor peroxisome

proliferator activated receptor gamma (PPARγ), modulation of reverse cholesterol transport, the inflammatory Iκk-NFκB kinase pathway, and endoplasmic reticulum (ER) stress, as well as manipulation of macrophage glucose metabolism through deleting GLUT1 to alter the inflammatory response (Erbay et al., 2009; Makowski, Brittingham, Reynolds, Suttles, & Hotamisligil, 2005).

Macrophages display tremendous heterogeneity regarding their functions and activities, reflecting their local metabolic and immune environment (Odegaard et al., 2007a). CAMs are pro-inflammatory and are formed through activation of the classical pathway when type 1 T-helper (Th1) inflammatory cytokines IFNγ and TNFα are induced by cytokines, gram negative bacterial endotoxin (LPS), or saturated FA stimulation. In contrast, AAM are activated by type 2 T-helper (Th2) cytokines IL-4 and IL-13 of the adaptive immune pathway. CAMs mount a robust inflammatory response combating infections, whereas AAMs are thought to be involved in remodeling and tissue repair through the production of IL-10, IL-1 receptor antagonist, and arginase-1 (Lumeng, Bodzin, & Saltiel, 2007). The skewing of AAM versus CAM levels in the vessel wall is as important as total number of infiltrating macrophages in the development of atherosclerosis (Chinetti-Gbaguidi & Staels, 2011; Leitinger & Schulman, 2013). Therefore, the purpose of this study is to address the gap regarding the knowledge of the mechanistic link between macrophage substrate metabolism and atherosclerosis development. Specifically, we focus on how macrophage glucose metabolism determines atherosclerotic plaque formation and morphology through affecting necrotic core and fibrous core formation.

Experimental Methods

Reagents

All reagents were purchased from Sigma-Aldrich (St. Louis, MO) unless otherwise noted. Carboxylate microspheres were obtained from Polysciences, Inc (Warrington, PA). Antibodies were purchased from the following sources: F4/80 (AbD Serotec/BioRad, CA); Annexin V PE Apoptosis Detection Kit PE (eBioscience, CA); Mouse IgG (Life technologies, CA); Goat anti-Mouse IgG, Rhodamine Red conjugate (Life technologies, CA); Goat Anti-Mouse IgG Cy5 (Life technologies, CA); Alexa Fluor oxL488 Phalloidin (Life technologies, CA). DL and acetyl LDL were purchased from Alfa Aesar Company (Ward Hill, MA). Fluoro-Gel II with DAPI was purchased from Electron Microscopy Sciences (Hatfield, PA). Glucometer and Glucose strips were purchased from Abbott Diabetes Care (Abbott Park, IL).

Animals and Maintenance

All animal experiments were performed in compliance with protocol approved by the University of North Carolina at Chapel Hill Institutional Animal Care and Use Committee. *Glut1*$^{fl/fl}$ mice were generously provided by Dr. Dale Abel (University of Iowa). LysM-Cre mice (stock number. 004781) and *Ldlr*$^{-/-}$ mice (stock number. 002207) were obtained from Jackson Laboratories (Bar Harbor, ME). *Glut1*$^{fl/fl}$ mice were backcrossed with C57BL/6J mice for 2 (Erbay et al., 2009) generations in the University of North Carolina at Chapel Hill animal facility and then crossed with LysM-Cre mice. All mice were housed in a12-hour light-dark cycle with *ad libitium* access to food and water. To generate littermate *Glut1*$^{fl/fl}$ and *Glut1*$^{M\Phi-/-}$ mice, male *LysM-Cre*$^{+/+}$ and female *Glut1*$^{fl/fl}$ mice were bred and kept *Glut1*$^{fl/fl}$*/LysM-Cre*$^{+/-}$ as breeders for experiments to generate littermates. Upon conducting BMT, chimeric *Ldlr*$^{-/-}$ mice were transferred to sterile cages with *ad libitium* access to sterile mouse chow and sterile water and

were maintained on chow diet for four weeks before challenge with WD (TD88137, 42% of Kcal from milk fat with 0.15% added cholesterol) from Harlan Teklad (Indianapolis, IN) for 12 weeks.

DNA isolation and GLUT1 genotyping

DNA was isolated from mouse-tail tissues or BMDMs using a DNeasy Blood and Tissue Kit (Qiagen, Valencia, CA) and DNA concentration was measured by NanoDrop 2000 (Thermo scientific, DE). Genotyping was performed using the following primers: Flanked loxP forward – CTGTGAGTTCCTGAGACCCTG; Flanked loxP reverse – CCCAGGCAAGGAAGTAGTTC; FRT forward: TCCATTCTCCAAACTAGGAAC; FRT-R2: GAAGGCACATATGAAACAATG. iProof High-Fidelity PCR super mix (Bio-Rad, Hercules, CA)-based genotyping was performed on a C1000 thermocycler (Bio-Rad, Hercules, CA).

Bone Marrow Transplantation

Upon arrival, 32 4-week-old male *Ldlr*$^{-/-}$ mice were randomized to two experimental groups (n=16). Each group received bone morrow from *Glut1*$^{fl/fl}$ or *Glut1*$^{M\Phi-/-}$ mice. At 6 weeks of age, recipient *Ldlr*$^{-/-}$ mice were administered two doses of X-ray irradiation (500cGy x 2, spaced 4 hours apart; X-RAD, North Branford, CT). *Glut1*$^{fl/fl}$ or *Glut1*$^{M\Phi-/-}$ donor mice were anesthetized by Tribromoethanol (TBE, 0.02 ml/g of a 1.25% solution) and afterward sacrificed by cervical dislocation. After removing surrounding connective tissues, the femur and tibia were collected and bone marrow cells were flushed by ice-cold PBS containing 2% bovine calf serum (Hyclone, UT). Bone marrows were passed through cell strainers to remove large residue and cell suspensions were centrifuged at 1200rpm at 4°C for 5 minutes. After removing medium, cell pellets were resuspended in HBSS buffer (Life technologies, CA). Each recipient mouse received

$5x10^6$ bone marrow cells through retro-orbital injection under anesthesia. Control animals were transplanted with the HBSS buffer only and died within 10 days of lethal irradiation.

Body weight and composition

Body weight was measured prior to starting mice on diet and weekly until sacrifice. Body composition including lean mass, fat mass, free water content, and total water content of non-anesthetized mice was measured at age of 5, 10, 16, and 22 weeks old using the EchoMRI-100 quantitative magnetic resonance whole body composition analyzer (Echo Medical Systems, Houston, TX). Fat mass or lean mass is presented as percent fat mass or lean mass over total body weight (Sundaram et al., 2013).

Histology and immunohistochemistry

Mice dissections were done as previously described but with minor modifications (Makowski et al., 2001a). Briefly, under the effects of anesthesia, left ventricles were perfused with PBS followed by 10% formalin and dissected out. Hearts with proximal aorta were fixed in 10% formalin for 24 hours. 16 hearts were transferred to 70% ethanol and stored at 4°C for future creation of formalin fixed paraffin embedded (FFPE) sections and 16 hearts were transferred to 30% sterile sucrose for 72 hours. Serial interrupted sections from FFPE hearts were cut at 5µm thickness. Serial sections from frozen sections were cut at 10µm thickness. FFPE sections were stained with Masson's trichrome for quantification of collagen content and necrotic cores. Frozen sections were stained with ORO and hematoxylin for quantification of lesion area.

Histology quantification

Quantification of atherosclerotic lesions was done as described with modification (Bjorkbacka et al., 2004; Rotllan et al., 2015). Serial interrupted sections were cut through the aorta at the origins of the aortic valve leaflets, and every other section (10 μm) throughout the aortic sinus (1600 μm) was stained with ORO and hematoxylin. Aortic lesion size of each animal was obtained by averaging 20 sections from the same mouse. 5μm serial interrupted sections were stained with Masson's trichrome and used for quantification of collagen content and necrotic cores. A color deconvolution algorithm, developed by Bentley Midkiff from UNC Translational Pathology Laboratory, was used to separate collagen for digital quantification. Scores of collagen amount were given based on the product of algorithm calculated as optical density (OD) x percent of total positive area stained with collagen. Necrotic cores were quantified by Aperio ePathology software after manually circling necrotic area.

Fasting Plasma Lipids

After 6 hours of fasting, 200μl blood was collected into an ETDA coated tube by submandibular bleeding. Blood was centrifuged at 10,000g for 2 minutes at 4°C; plasma was then transferred to another tube. Plasma was diluted to 1:10 with PBS. From this diluted plasma, total cholesterol, HDL-cholesterol, and triglycerides were measured in the UNC Animal Clinical Chemistry and Gene Expression Core Facility by Vt350 automated chemical analyzer from Ortho-Clinical Diagnostics Company (Rochester, NY).

Blood Pressure

Blood pressure was measured as described previously (Zhou et al., 2012) with minor modifications using a tail-cuff system in UNC Rodent Advanced Surgical Models Core Lab.

Mice (n=8) received 5 consecutive days of training on the tail-cuff blood pressure system (CODA, Kent Scientific, CA) prior to data collection. Starting on day 6, systolic and diastolic blood pressure was measured in conscious mice daily for 3 days. Mice were acclimated to the warm (32°C) restrainer for 15 minutes and blood pressure was recorded during 10 acclimation followed by 25 measurement cycles.

Cell culture

All cultures were maintained under a fully humidified atmosphere of 95% air and 5% CO_2 at 37°C. Mouse thioglycollate-elicited macrophages were obtained as described (Makowski et al., 2001b; Zhang, Goncalves, & Mosser, 2008). 4% brewer thioglycollate was sterilized by autoclave and stored at -80°C for at least 3 months before use. On day 0, mice were injected with 1 ml of sterile 4% thioglycollate in the peritoneal cavity. The sterile-inflammatory response was then allowed to proceed for 4 days. On day 4, mice were euthanized using a carbon dioxide chamber followed by cervical dislocation. Before making a small incision, the abdominal area of each mouse was cleaned with 70% ethanol. Then, 5ml of cold sterile PBS was injected into the peritoneal cavity, taking care not to puncture internal organs. The PBS was gently spread into the whole abdominal cavity and the same syringe was used to aspirate a cell suspension from the left side of the abdomen into a 50ml Falcon tube. The cell suspension was centrifuged at 1000rpm for 10 minutes at 4°C, followed by aspiration of the supernatant and lysis of red blood cells by ACK lysing buffer (Lonza, MD). The AKC buffer was neutralized by adding 13ml of RPMI cell media supplemented with 10% FBS, 1X L-glutamine, and 1X penicillin/streptomycin antibiotic mix (Corning, NY). Next, the cell suspension was again centrifuged at 1000rpm for 10 minutes at 4°C, the supernatant was aspirated, 3 ml of RPMI was added into the cell pellet, and the cells

were counted. Finally, the cells were diluted into different concentrations for plating 6-well and 24-well plates.

Phagocytosis assay

Coverslips were coated in a 24-well plate with 1ml of 10µg/ml rat tail collagen I (Corning, NY) overnight in a sterile cell culture hood. Collagen-coated coverslips were then washed with sterile PBS twice and air dried. Mouse peritoneal macrophages were seeded at a concentration of $8x10^5$ cells per well and left to attach to coverslips overnight. The carboxylated microspheres were opsonized with normal mouse IgG by mixing 3 ml of sterile PBS, 60µl of microspheres, and 60µl of mouse IgG and rotating this suspension at 37°C for one hour. Suspensions were centrifuged at 1600rpm for 10 minutes at 4°C, the supernatants were removed by aspiration, and the microspheres were resuspended in 3 ml of cold PBS and centrifuged at 1600rpm for another 10 minutes at 4°C. After removing the supernatant, the microsphere pellet was resuspended in a final 200µl of cold PBS. 25µl of microsphere suspension was loaded into each well and after 20 minutes of incubation, phagocytosis was stopped by washing off non-internalized microspheres with room temperature PBS three times for 10 minutes each time. Cells were fixed in 4% paraformaldehyde at room temperature for 10 minutes then washed with PBS three times for10 minutes. Cells were blocked by adding a blocking buffer of 1:1 ratio of 10% BSA: 10% normal goat serum for 30 minutes. 250µl goat anti-Mouse rhodamine red-X 1:750 in 1% BSA was added to each well for 15 minutes then cells were washed for 5 minutes three times by PBS. Cells were permeabilized in 0.1% Triton X-100 for 5 minutes and were washed 3 times by PBS, then blocked by the same blocking buffer for another 30 minutes. Goat anti-Mouse Cy5 and Alexa 488-Phalloidin, both 1:500 in 1% BSA, were added to wells for 30 minutes and then cells were washed twice for 5 minutes in PBS. Coverslips were gently removed

from wells and mounted to slides with Fluoro-Gel II with DAPI (Electron Microscopy Sciences, PA) mounting media for future analysis. ZEISS LSM 700 confocal microscope (UNC Microscopy service lab) was used to capture the images. Phagocytosis Index (PI) was calculated by numbers of microspheres took up by cells divided by total microspheres in the field. Results from 5 fields were averaged.

Statistics

For all *in vivo* and *ex vivo* data, statistical differences between experimental groups were determined by unpaired Student's *t*-tests using statistical software within GraphPad Prism (GraphPad Software, Inc., La Jolla, CA). All data are shown as mean ± standard error of the mean (SEM). P values less than 0.05 were considered statistically significant.

Results

Deletion of macrophage GLUT1 did not alter metabolic parameters in *Ldlr*$^{-/-}$ mice

Weekly body weight excluding 2 weeks after BMT and body composition including before BMT, before diet, and 6 weeks on diet and 12 weeks on diet were measured to determine if abolishing glucose metabolism in macrophages affects systemic metabolic parameters of *Ldlr*-/- mice. In addition, fasting blood glucose was measured every 3 weeks and fasting total cholesterol, HDL cholesterol, and triglyceride in plasma was measured at 12 weeks on WD. *Glut1*$^{M\Phi+/+}$ *Ldlr*$^{-/-}$*and Glut1*$^{M\Phi-/-}$ *Ldlr*$^{-/-}$ mice body weights did not differ after a 12 weeks WD exposure (Figure 5). Likewise, fat and lean muscle percentages were not significantly different between *Glut1*$^{fl/fl}$ *Ldlr*$^{-/-}$ and *Glut1*$^{M\Phi-/-}$ *Ldlr*$^{-/-}$ mice (Figure 6 A-B). Interestingly, circulating total cholesterol and LDL cholesterol concentrations in plasma were significantly higher in *Glut1*$^{M\Phi-/-}$ *Ldlr*$^{-/-}$ mice compared to *Glut1*$^{fl/fl}$ *Ldlr*$^{-/-}$ mice (Figure 7 A-B, p=0.0196 and p=0.0171). There

were no differences in plasma HDL cholesterol or triglycerides (Figure 8 A-B). Additionally, systolic and diastolic blood pressure was recorded at the age of 16 weeks of age, but there was no genotype effect (Figure 9 A-B). In addition, 6-hour fasting glucose was recorded at 5, 10, 13, 16, 19, and 22 weeks of age with no GLUT1- mediated differences detected (Figure 10).

Lack of macrophage GLUT1 does not affect atherosclerosis lesion size

Preliminary data from the Makowski Lab indicated that *Glut1*$^{MΦ-/-}$ BMDMs failed to elicit a pro-inflammatory response. *Glut1*$^{MΦ-/-}$ expressed 80% less IL-1β and 60% less iNOS messenger RNA compared to *Glut1*$^{fl/fl}$ BMDMs. We sought to understand whether GLUT1-mediated modulation of the macrophage inflammatory phenotype could reduce atherosclerotic plaque size since atherosclerosis is dependent on inflammation. To achieve our purpose, we conducted BMT by transplanting bone marrow collected from *Glut1*$^{MΦ-/-}$ or *Glut1*$^{fl/fl}$ mice or vehicle control HBSS buffer into *Ldlr*$^{-/-}$ mice through retro-orbital injection. After 12 weeks of WD exposure, we assessed aortic root lesion formation by histology. All mice that received vehicle transplantation died at 10 or 11 days post-irradiation, while all of the mice that received BMT survived. At the end point of the experiments, when mice were 22 weeks of age, we assessed lesion size by quantifying the average of lesion areas/section in both groups. After analyzing ORO stained aortic sinus lesions, we observed no difference in lesion size between *Glut1*$^{fl/fl}$ *Ldlr*$^{-/-}$ and *Glut1*$^{MΦ-/-}$ *Ldlr*$^{-/-}$ mice (Figure 11 A-C).

***Glut1*$^{MΦ-/-}$ *Ldlr*$^{-/-}$ chimeric mice develop fewer and smaller necrotic cores than *Glut1*$^{fl/fl}$ *Ldlr*$^{-/-}$ mice**

Ldlr$^{-/-}$ mice develop advanced atherosclerotic lesions after a 12 weeks of high cholesterol diet (Subramanian, Thorp, & Tabas, 2015). Advanced lesions are characterized by increased cell

death and necrotic core formation. We next sought to investigate whether abolishing glucose metabolism in macrophages affected the necrotic area. We analyzed Masson's trichrome stained FFPE sections (Figure12 A-B) and observed more than a 50% increase in the necrotic area in the *Glut1*$^{MΦ-/-}$ *Ldlr*$^{-/-}$ mice compared to *Glut1*$^{fl/fl}$ *Ldlr*$^{-/-}$ mice (Figure 12 C). 87.5% (7 out of 8) of *Glut1*$^{MΦ-/-}$ *Ldlr*$^{-/-}$ mice developed necrosis but only 37.5% (3 out of 8) *Glut1*$^{fl/fl}$ *Ldlr*$^{-/-}$ mice developed a necrotic core (Figure 12 D).

Deletion of macrophage GLUT1 decreased collagen amount in aorta sinus

Collagen is majorly secreted by lesion SMCs. MMP, secreted by pro-inflammatory macrophages and necrotic foam cells, degrades collagen and increases lesion vulnerability. Surprisingly, we observed a 20% decrease in collagen content in the aorta sinus of *Glut1*$^{MΦ-/-}$ *Ldlr*$^{-/-}$ mice compared to *Glut1*$^{fl/fl}$ *Ldlr*$^{-/-}$ mice (Figure 13 A-B, p=0.0161 and p=0.0065).

Lack of GLUT1 decreased macrophage phagocytic capacity

Necrotic cores in atherosclerotic lesions largely result from an imbalance between decreased lesion efferocytosis and increased foam cell apoptosis. Having observed a striking difference in the necrotic areas between *Glut1*$^{fl/fl}$ and *Glut1*$^{MΦ-/-}$ mice, we set out to test how deletion of GLUT1 affects macrophage phagocytic capacity in a phagocytosis assay using peritoneal macrophages isolated from *Glut1*$^{fl/fl}$ and *Glut1*$^{MΦ-/-}$ mice (Figure 14 A-B). Phagocytosis Index (PI) was 69.7% and 57.2% respectively in *Glut1*$^{fl/fl}$ and *Glut1*$^{MΦ-/-}$ macrophages (Figure 14 C, p=0.013). *Glut1*$^{MΦ-/-}$ macrophages had 16.3% reduction of their phagocytic capacity relative to *GLUT1*$^{fl/fl}$ macrophages.

Discussion

A body of evidence has demonstrated that macrophages are implicated in chronic adipose tissue inflammation, obesity, insulin resistance, and T2D. Macrophage metabolism and the immune response are closely intertwined with each other (Odegaard & Chawla, 2011). The link between fatty acid oxidation and macrophage alternative activation has been elucidated (Odegaard et al., 2007b; Vats et al., 2006). However, the role of glucose metabolism in regulating macrophage polarization is still poorly understood. GLUT1 is the predominant glucose transporter on macrophages (Freemerman et al., 2014). In order to understand how glucose metabolism affects macrophage polarization, our lab created a mouse macrophage RAW 246.7 cell line which stably over-expressed GLUT. Freemerman et al. demonstrated that over-expression of GLUT1 significantly increased glucose uptake, lactate production, and simultaneously TNF-α, IL-1β, IL-6, and PAI-1 gene expression, in a glycolysis and ROS-dependent manner, indicating that glucose metabolism plays a key role in driving macrophage to mount a robust, pro-inflammatory response (Freemerman et al., 2014). We generated a novel *Glut1*$^{M\Phi-/-}$ mouse model wherein *Glut1* was specifically deleted from hematopoietic myeloid cells using LysM-Cre. Preliminary data demonstrated that lack of GLUT1 decreased iNos and IL-1β gene expression in BMDMs. In addition, *Glut1*$^{M\Phi-/-}$ mice made obese by HFD displayed elevated macrophage infiltration and crown like structure formation in epididymal white adipose compared to *Glut1*$^{fl/fl}$ mice, yet a striking lack of inflammation was evident, despite greater macrophage infiltration. Macrophage in white adipose of *Glut1*$^{M\Phi-/-}$ mice were polarized towards the AAM phenotype, despite being in a state of obesity with excessive macrophage infiltration (manuscript in preparation). Taken together, the data suggests that glucose is the primary fuel metabolized by pro-inflammatory macrophages (Freemerman et al., 2014). Since macrophages

play a central role in the pathogenesis of atherosclerosis, and because obesity and atherosclerosis share certain common etiologies such as chronic inflammation, we intended to expand our knowledge garnered from the *in vitro* GLUT1 gain of function model and the *in vivo* GLUT1 loss of function obesity mouse model to investigate how macrophage glucose metabolism affects atherosclerosis. We chose to use atherogenic $Ldlr^{-/-}$ mice as bone marrow recipient mice because transplanting $ApoE^{+/+}$ macrophages into $ApoE^{-/-}$ mice decelerates atherogenesis in $ApoE^{-/-}$ mice (Getz & Reardon, 2012). Our initial hypothesis was that mice with mutated macrophage glucose metabolism would develop reduced atherosclerosis because of decreased macrophage pro-inflammatory response. However, after 12 weeks of WD exposure, deletion of macrophage GLUT1 surprisingly did not affect atherosclerotic lesion size per se but strikingly altered the composition of lesions compared to floxed controls. Lack of macrophage GLUT1 increased necrotic core formation and decreased aorta sinus collagen content.

We showed that deletion of macrophage GLUT1 did not affect $Ldlr^{-/-}$ mouse body weight or fasting glucose. We also did not observe any difference on other systemic measurements including body composition, blood pressure, plasma HDL cholesterol, and plasma triacylglycerol. Of note, $Glut1^{M\Phi-/-}$ $Ldlr^{-/-}$ mice fed 12 weeks of WD had significantly higher plasma total cholesterol and LDL cholesterol than $Glut1^{fl/fl}$ $Ldlr^{-/-}$ mice. Plasma cholesterol concentration is determined by endogenous cholesterol synthesis, dietary intake, and clearance. All mice received WD during the 12-week diet exposure; therefore it was likely that deletion of macrophage GLUT1 affected liver cholesterol synthesis or secretion. Our preliminary data indicated that $Glut1^{M\Phi-/-}$ mice developed more crown like structure (CLS) than $Glut1^{fl/fl}$ mice in epididymal white adipose tissue when mice were made obese on a HFD. The elevated macrophage influx as measured by CLS, qPCR, and flow cytometry was likely due to increased

expression of MCP-1 in *Glut1*$^{MΦ-/-}$ adipose tissue; MCP-1 expression was 70-fold higher in *Glut1*$^{MΦ-/-}$ epididymal white adipose compared to *Glut1*$^{fl/fl}$ adipose tissue. One explanation for increased plasma total cholesterol and LDL cholesterol is that deletion of macrophage GLUT1 could have increased macrophage liver infiltration, and consequently increased total activity of pro-inflammatory cytokines such as IL-1β. It is well established that pro-inflammatory cytokines, including TNF-α, IL-1β, and IL-6, increase hepatic *de novo* cholesterol and lipogenesis (Popa, Netea, van Riel, van der Meer, & Stalenhoef, 2007; Zhao et al., 2011).

Phagocytosis is the process of engulfing particles larger than 0.5μm and requires receptor participation. Macrophages play critical roles in defending against infection, maintaining tissue homeostasis, and remodeling through phagocytizing foreign bodies such as bacteria, fungi, and apoptotic bodies. Cells undergoing apoptosis release various molecules such as ATP, lysophosphatidylcholine, and sphingosine 1-phosphate which function as chemokines, recruiting phagocytes to the vicinity of dying cells (Flannagan, Jaumouille, & Grinstein, 2012). Venter et al. demonstrated that glycolysis fuels LPS-induced macrophage cell shape changes and phagocytosis of zymosan particles in the RAW macrophage 246.7 cell line, which highlights the role of glucose in maintaining functional macrophage phagocytosis (Venter et al., 2014). Unabatedly engulfment of oxLDL renders macrophages susceptible to apoptosis. If phagocytes are able to effectively clear the apoptotic bodies, the extent of secondary necrosis and necrotic cores would largely reduce, conversely decreased phagocytosis results in increased necrotic core formation. 6-Phosphofructo-2-kinase/fructose-2, 6-biphosphatase 3 (PFKFB3) regulates the rate-limiting step of the glycolysis pathway. Nishizawa et al. showed that knocking down GLUT1 by siRNA decreased PFKFB3 gene expression (Nishizawa et al., 2014). Besides its important role in glycolysis, PFKFB3 also regulates actin cytoskeleton remodeling (De Bock et al., 2013).

Therefore we speculated that lack of GLUT1 decreased PFKFB3 activity which further reduced actin cytoskeleton remodeling in macrophages. Macrophages with reduced ability to rearrange actin cannot form proper pseudopodia, and therefore phagocytic capacity is impaired (Coppolino et al., 2002). In the subendothelium space of blood vessels, decreased macrophage phagocytic capacity eventually leads to necrotic core formation in atherosclerotic lesion.

To characterize the effect of GLUT1 on phagocytic capacity, we performed an *ex vivo* phagocytosis assay to test the capacity of thioglycollate-elicited peritoneal macrophages to phagocytose normal mouse IgG opsonized 2μm microspheres as a model of engulfing Lipoproteins. Results of the pilot study suggested that *Glut1*$^{M\Phi-/-}$ macrophages displayed reduced phagocytic capacity relative to *Glut1*$^{fl/fl}$ macrophages. These findings corroborated our findings on histologic quantification of necrotic cores. Furthermore, preliminary data in diet-induced obese mice suggested that although macrophages infiltrated in greater numbers in *Glut1*$^{M\Phi-/-}$ mice, they failed to polarize to CAMs. One hypothesis is that the macrophages infiltrate but fail to activate because of a lack of phagocytic capacity of macrophages lacking GLUT1. We also observed decreased collagen content in *Glut1*$^{M\Phi-/-}$ *Ldlr*$^{-/-}$ mice compared to *Glut1*$^{fl/fl}$ *Ldlr*$^{-/-}$ mice which may have resulted from increased MMP released by necrotic *Glut1*$^{M\Phi-/-}$ foam cells. **Taken together, we have provided preliminary data that macrophage GLUT1 is required to maintain the functional phagocytic capacity and therefore sustain atherosclerotic lesion stability.**

A recent study also examined macrophage GLUT1 by gain of function strategy. By transplanting *Ldlr*$^{-/-}$ mice with macrophages overexpressing GLUT1, Nishizawa et al. reported that increasing macrophage glucose metabolism by over-expressing GLUT1 did not affect atherosclerosis. They demonstrated that there was no difference in atherosclerosis lesion size and

necrotic areas between GLUT1 overexpressed macrophage and wild type macrophage transplanted *Ldlr*$^{-/-}$ mice (Nishizawa et al., 2014). This was the first article to document the role of macrophage glucose metabolism in atherosclerosis. Our results were consistent with their finding that altering macrophage glucose metabolism did not affect atherosclerotic lesion size, but by utilizing a loss of function model we observed that mice with deleted macrophage GLUT1 developed more and larger necrotic core areas in atherosclerotic lesions. **We speculate that overexpression of macrophage GLUT1 either maintains or increases PFKFB3 activity and as a result, decreased macrophage phagocytic capacity was not seen in Nishizawa's study.**

In summary, deletion of macrophage GLUT1 increased plasma total cholesterol and LDL cholesterol but did not affect body weight, body composition, or fasting glucose. In the aorta sinus, more and larger necrotic cores but less collagen content were observed in *Glut1*$^{M\Phi-/-}$ mice. We hypothesize that deletion of macrophage GLUT1 may have increased liver lipogenesis and furthermore that maintenance of atherosclerotic lesion stability may be regulated by macrophage specific glucose-dependent mechanisms. In order to test our hypothesis we will measure total lipid content in liver from frozen liver tissues; also stain liver FFPE sections with macrophage surface marker F4/80 to examine liver macrophage infiltration. In future studies, we aim to repeat *ex vivo* phagocytosis assays and further measure whether deletion of GLUT1 increases macrophage apoptosis. Last, we will stain aorta sinus sections with Mouse Macrophages/Monocytes antibody (Moma-2) to quantify aorta root macrophage infiltration. Taken together, this study provides evidence for the first time that macrophage GLUT1-dependent glucose metabolism plays a critical role in maintaining atherosclerotic lesion stability.

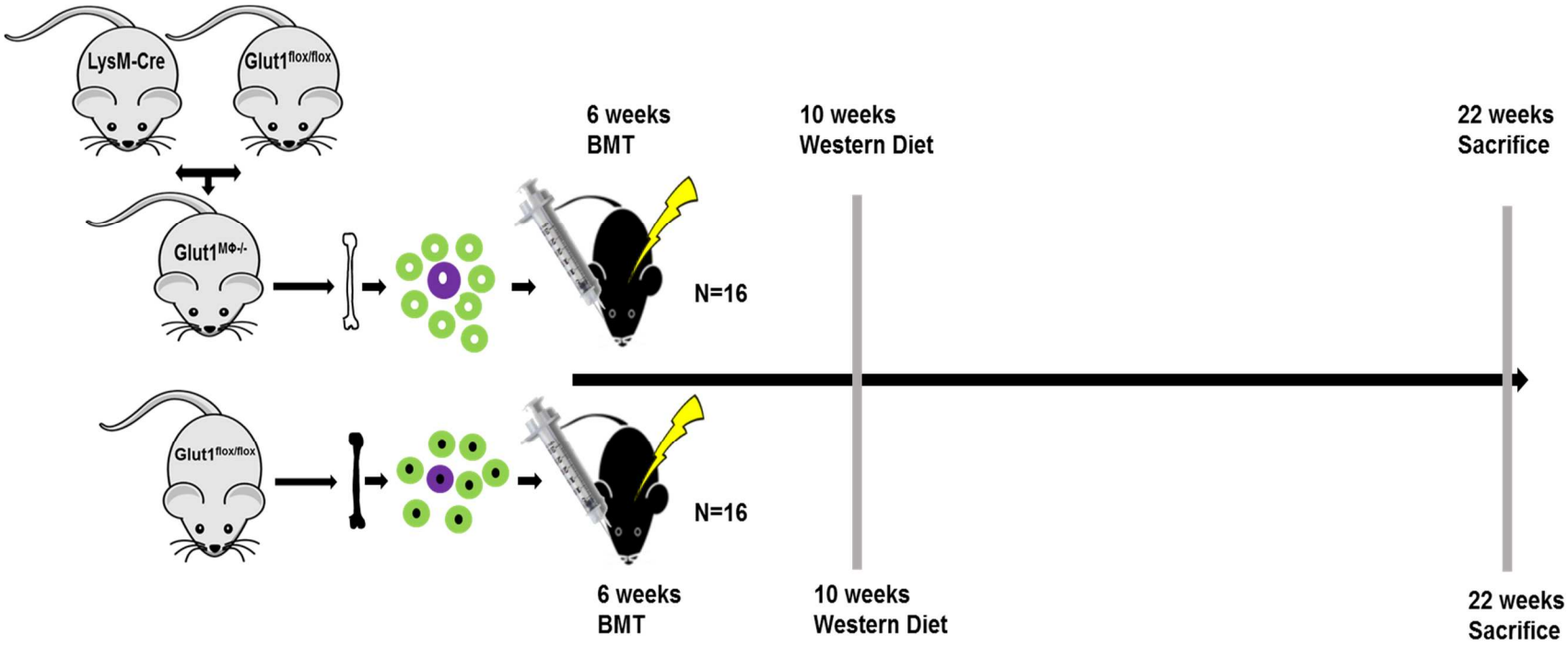

Figure 4. Diagram of Study Design. Littermate male *Glut1*$^{fl/fl}$ and *Glut1*$^{MΦ-/-}$ donor mice were maintained at the UNC animal facility. Recipient male *Ldlr*$^{-/-}$ mice were purchased from Jackson laboratory at 4 weeks of age. At 6 weeks of age *Ldlr*$^{-/-}$ mice were lethally irradiated and transplanted with 5x10^6 bone marrow cells which were collected from sex- and age-matched donor mice. Chimeric *Ldlr*$^{-/-}$ mice were reconstituted for 4 weeks before being exposed to WD for 12 weeks. At the age 22 weeks, mice were sacrificed.

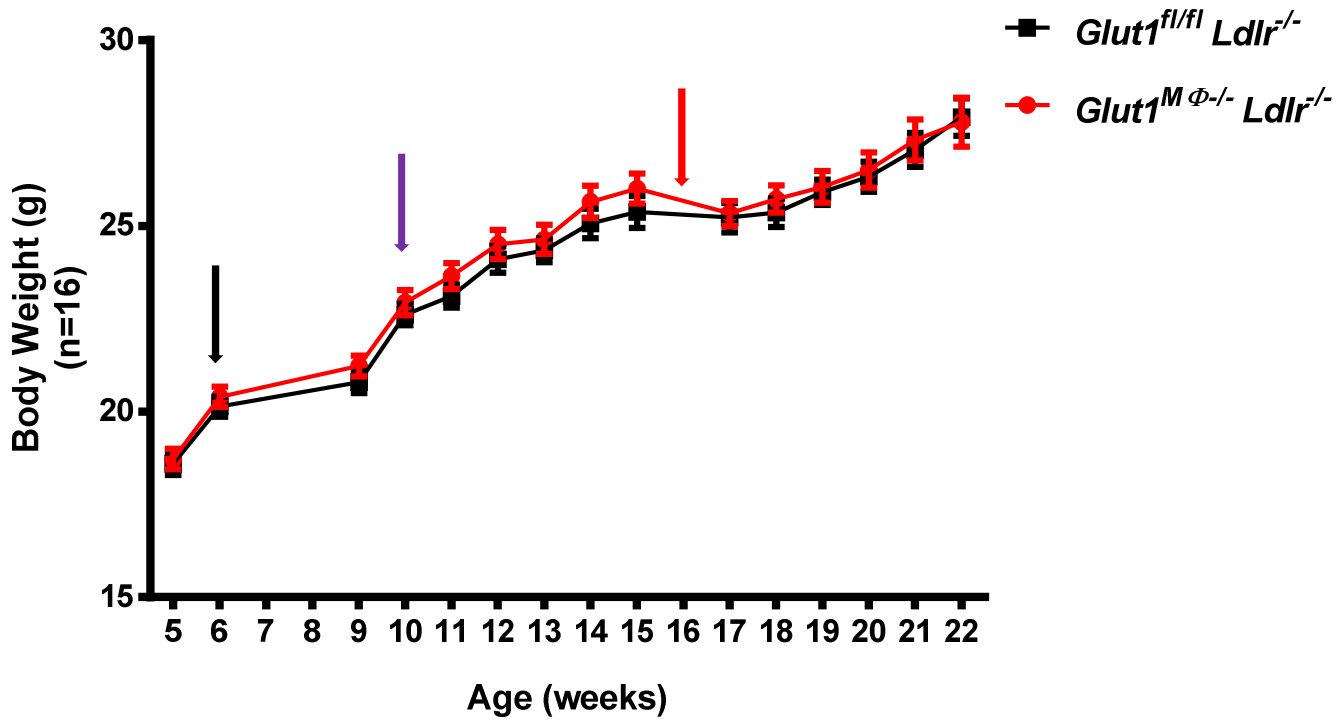

Figure 5. Deletion of macrophage GLUT1 did not increase *Ldlr*$^{-/-}$ mice's susceptibility to weight gain. Body weights of *Ldlr*$^{-/-}$ mice were measured weekly starting at 5 weeks of age. Irradiation and BMT occurred at 6 weeks of age (black arrow). WD started at 10 weeks of age (purple arrow). Blood pressure was measured at 16 weeks of age (red arrow) (n=16 per *Glut1* genotype).

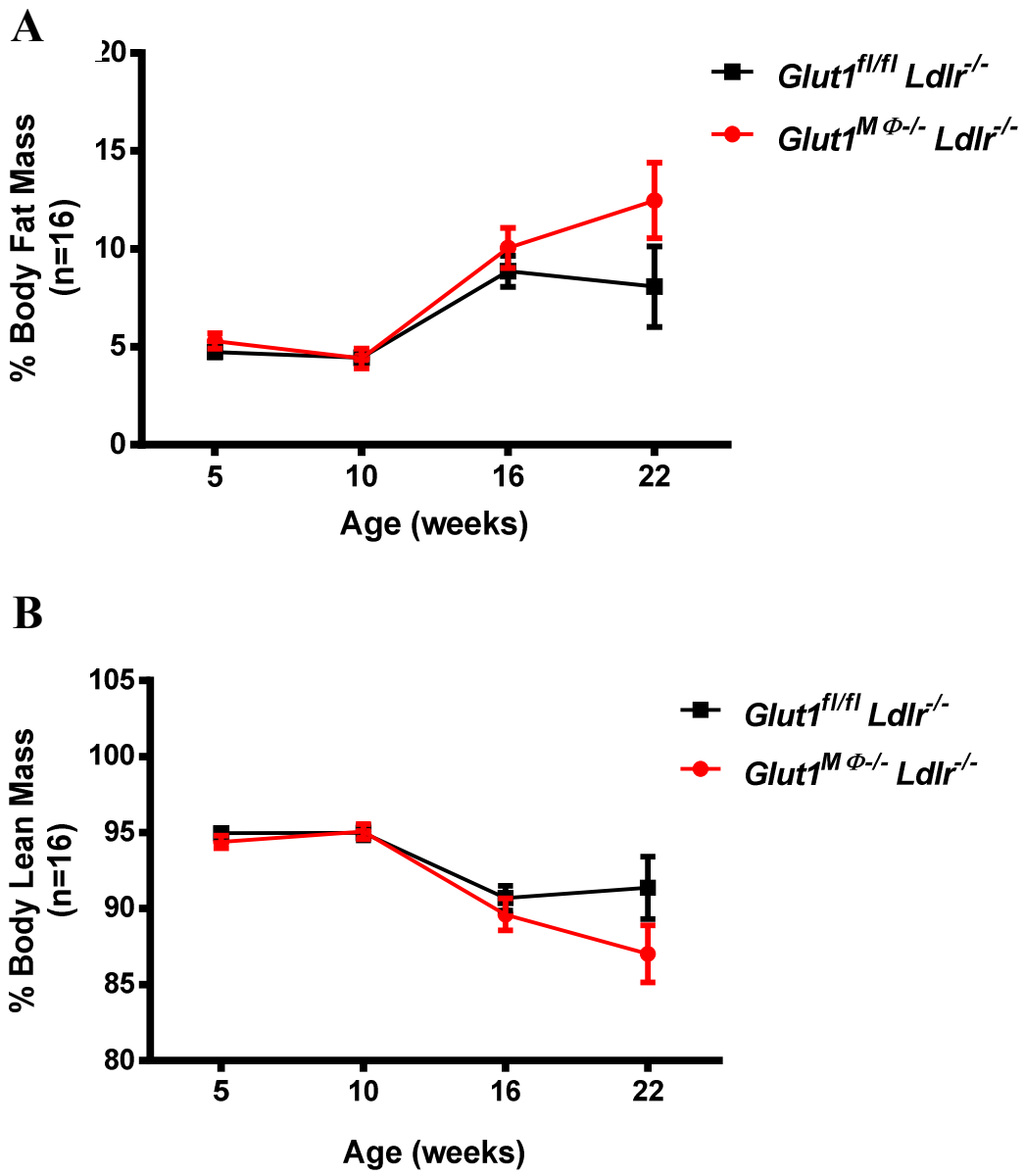

Figure 6. Deletion of macrophage GLUT1 did not alter body composition in recipient *Ldlr*$^{-/-}$ mice. (A) Body fat mass and (B) lean mass percentage were measured by Echo MRI at 5, 10, 16, and 22 weeks of age corresponding to before BMT, before diet, 6 weeks on diet, and 12 weeks on diet (at sacrifice). Data are presented as means ± SEM, n = 16 per *Glut1* genotype.

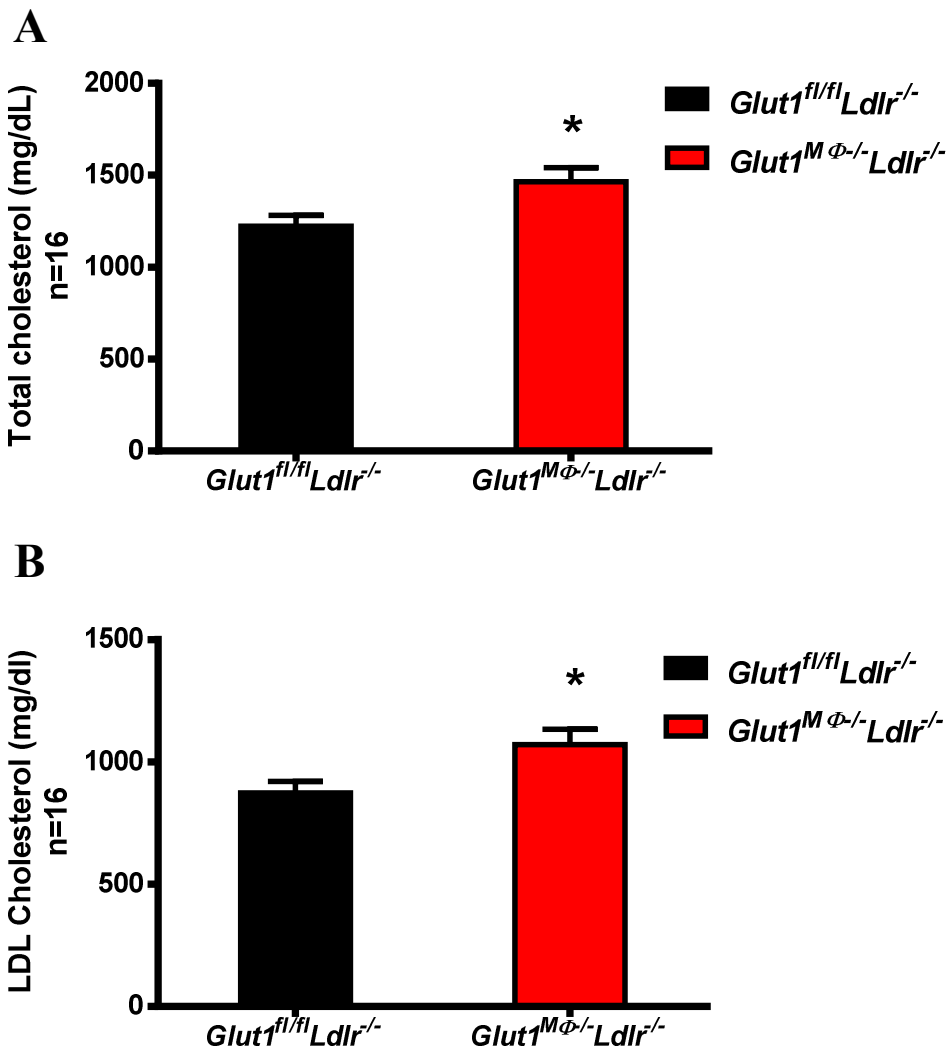

Figure 7. Lack of macrophage GLUT1 increased plasma total cholesterol and LDL cholesterol. Six hour fasted plasma lipids at 22 weeks of age were measured in the UNC Animal Clinical Chemistry and Gene Expression Core Facility. (A) Total cholesterol was 1464±77 mg/dl for *Glut1$^{MΦ-/-}$Ldlr$^{-/-}$* mice, and 1223 ± 59.07 mg/dl for the *Glut1$^{fl/fl}$ Ldlr$^{-/-}$ mice. (*P<0.05). (B) LDL cholesterol was calculated by subtracting HDL cholesterol from total cholesterol. LDL cholesterol were 1071 ± 62.62 mg/dl for the *Glut1$^{MΦ-/-}$Ldlr$^{-/-}$* mice, and 873.1 ± 46.93 mg/dl for the *Glut1$^{fl/fl}$ Ldlr$^{-/-}$ mice. (*P<0.05*). Data are presented as means ± SEM, n = 16 per *Glut1* genotype.

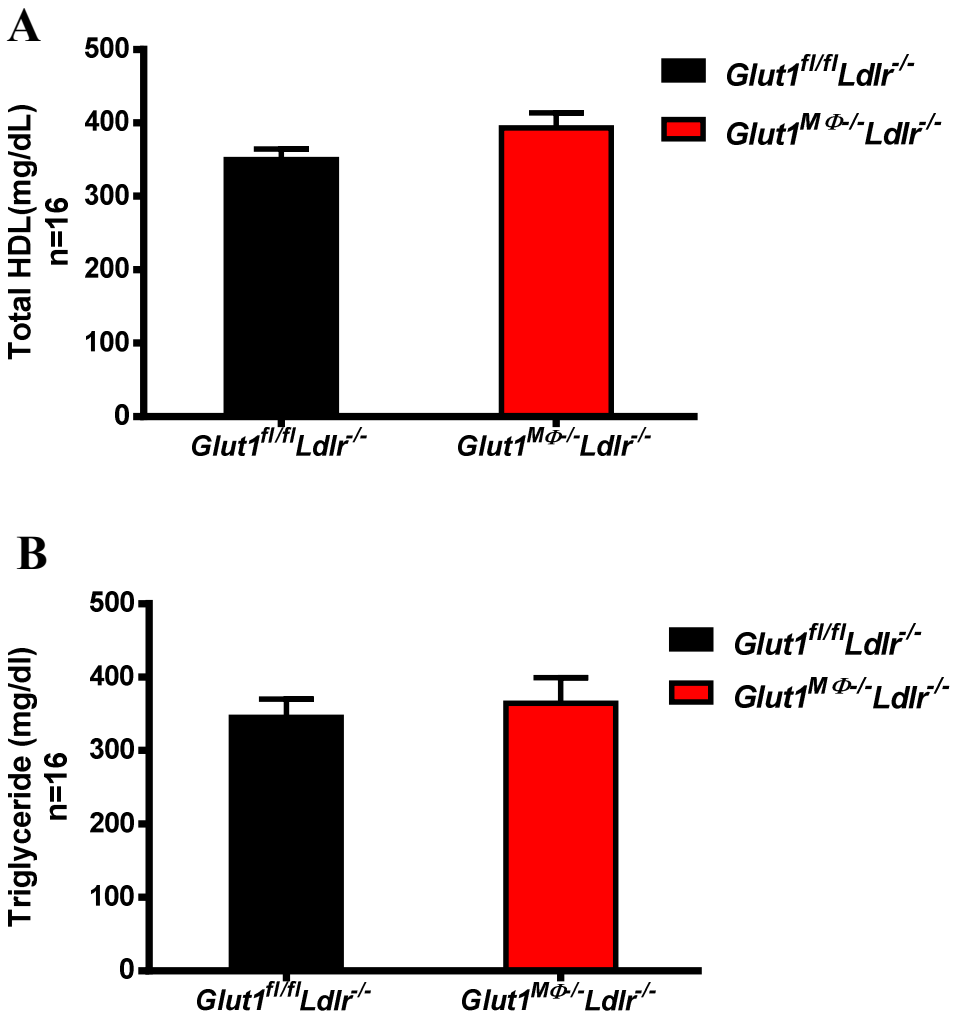

Figure 8. Lack of macrophage GLUT1 did not alter plasma HDL cholesterol and triacylglycerol. (A) 6 hours fasted plasma HDL and (B) triacylglycerol were measured in UNC Animal Clinical Chemistry and Gene Expression Core Facility as above. Data are presented as means ± SEM, n = 16 per *Glut1* genotype.

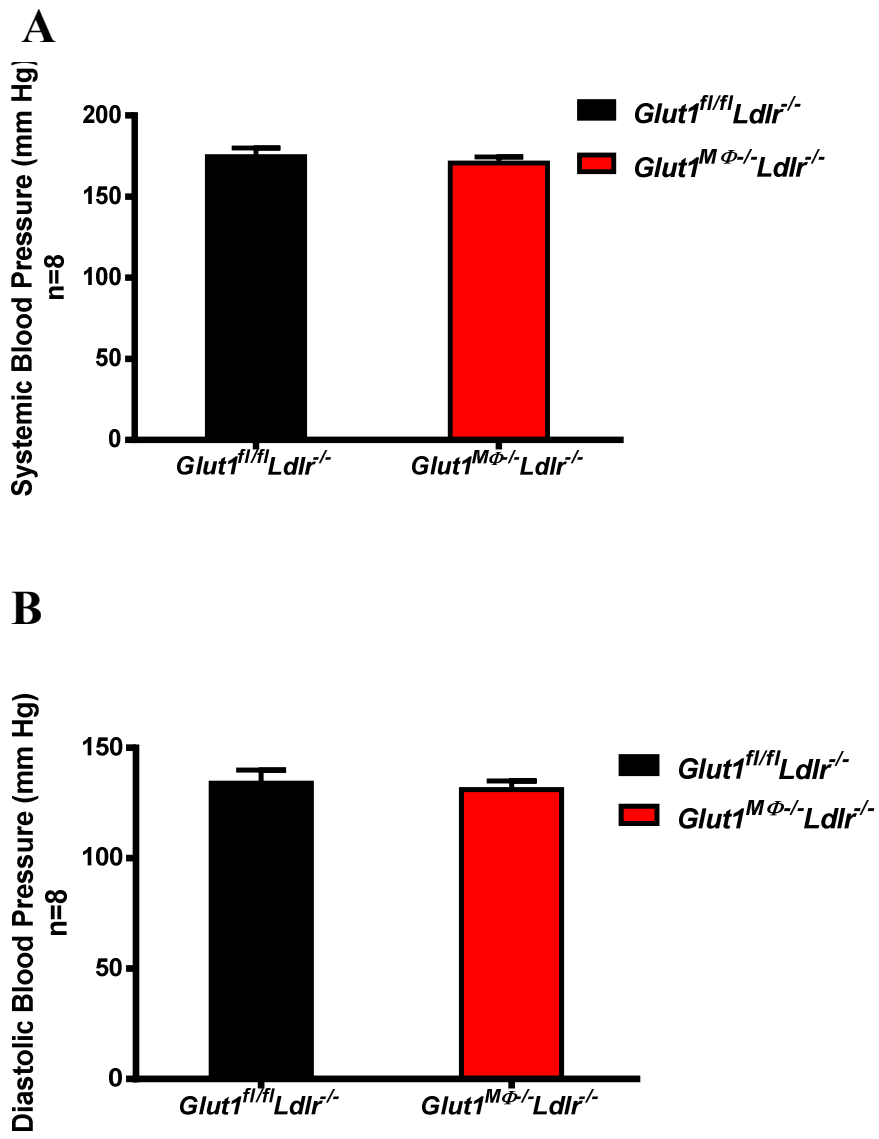

Figure 9. Deletion of macrophage GLUT1 did not change blood pressure after 6 weeks on WD. Blood pressure was measured at 16 weeks of age using a tail-cuff system. (A) Systolic and (B) diastolic blood pressure were measured in *Glut1*$^{MΦ-/-}$*Ldlr*$^{-/-}$and *Glut1*$^{fl/fl}$ *Ldlr*$^{-/-}$ mice. Data are presented as means ± SEM, n = 8 per *Glut1* genotype.

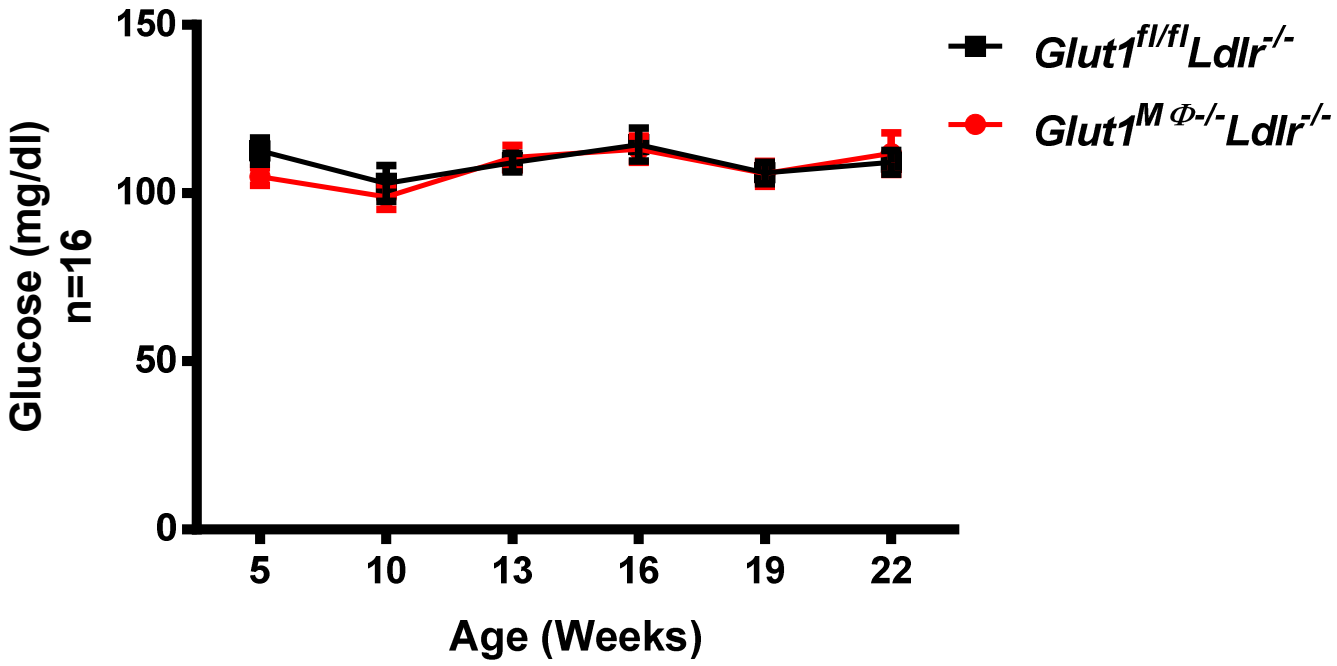

Figure 10. Lack of macrophage GLUT1 did not change fasting plasma glucose. 6 hours fasted glucose was measured at indicated time points in *Glut1*$^{M\Phi-/-}$*Ldlr*$^{-/-}$and *Glut1*$^{fl/fl}$ *Ldlr*$^{-/-}$ mice. Data are presented as means ± SEM, n = 16.

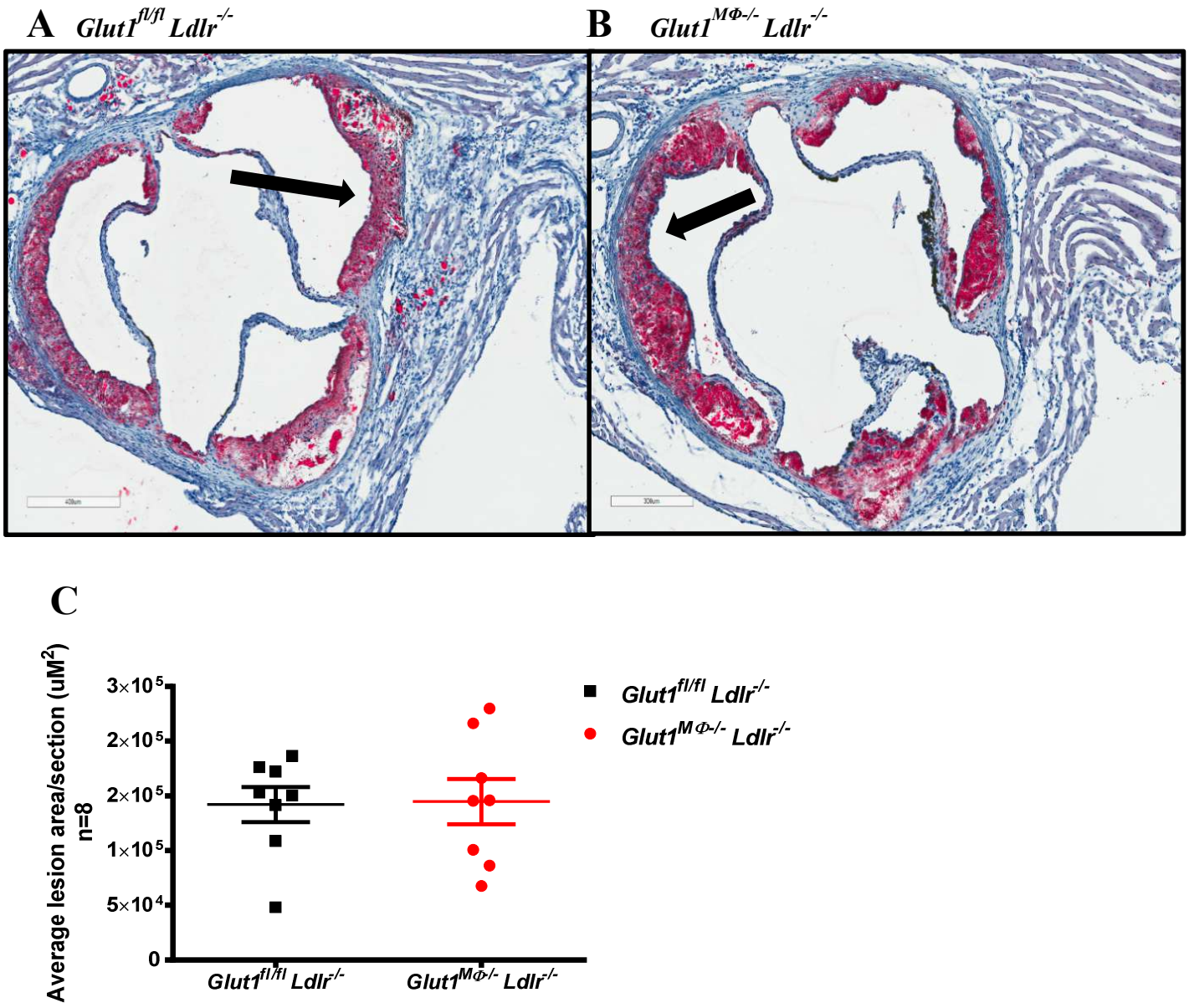

Figure 11. Deletion of macrophage GLUT1 did not affect atherosclerotic lesion size in the aorta sinus. Serial interrupted 10µm sections were stained with ORO and counter stained with Hematoxylin. Slides were scanned by Aperio Digital Slides Scanner. (A-B) 20X representative photomicrographs of ORO staining. Black arrow indicates representative lesions quantified. (C) Quantitative analysis of atherosclerotic lesion size in *Glut1*$^{fl/fl}$ *Ldlr*$^{-/-}$or *Glut1*$^{MΦ-/-}$*Ldlr*$^{-/-}$ mice. Data are presented as means ± SEM, n = 8 per *Glut1* genotype.

A ***Glut1$^{fl/fl}$ Ldlr$^{-/-}$***

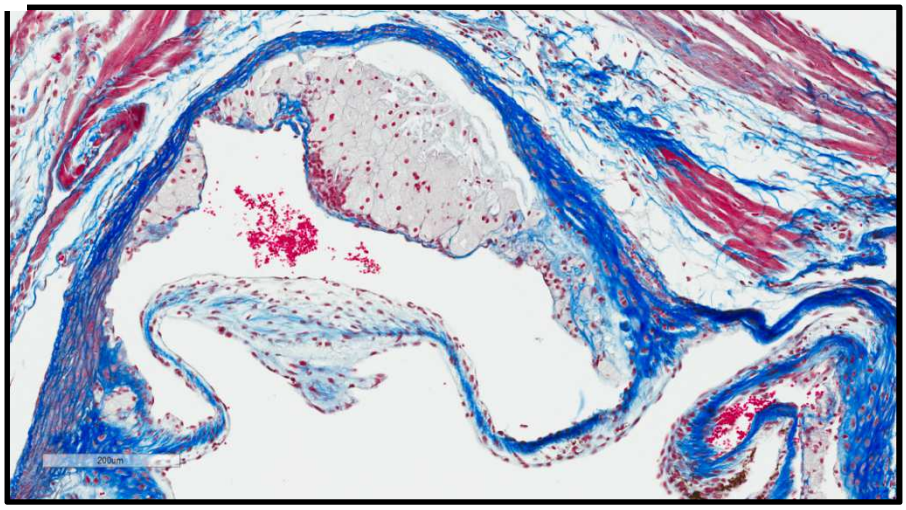

B ***Glut1$^{MΦ-/-}$ Ldlr$^{-/-}$***

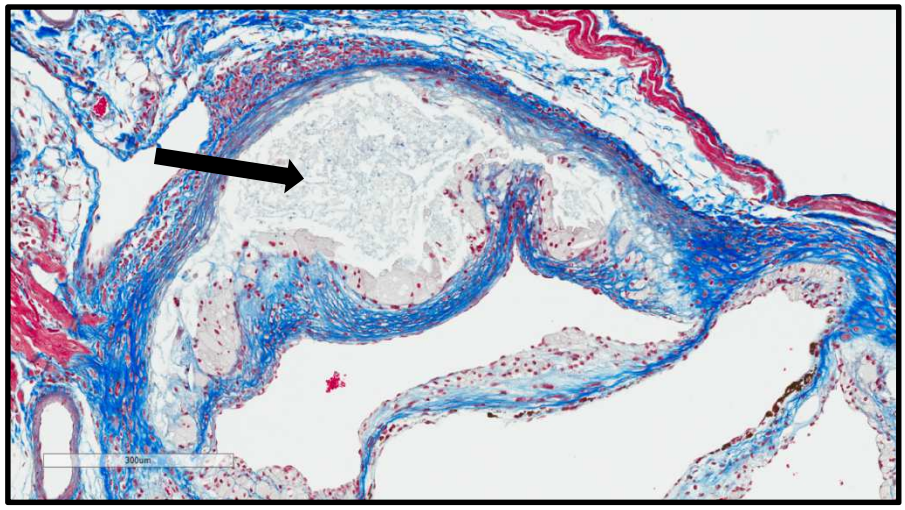

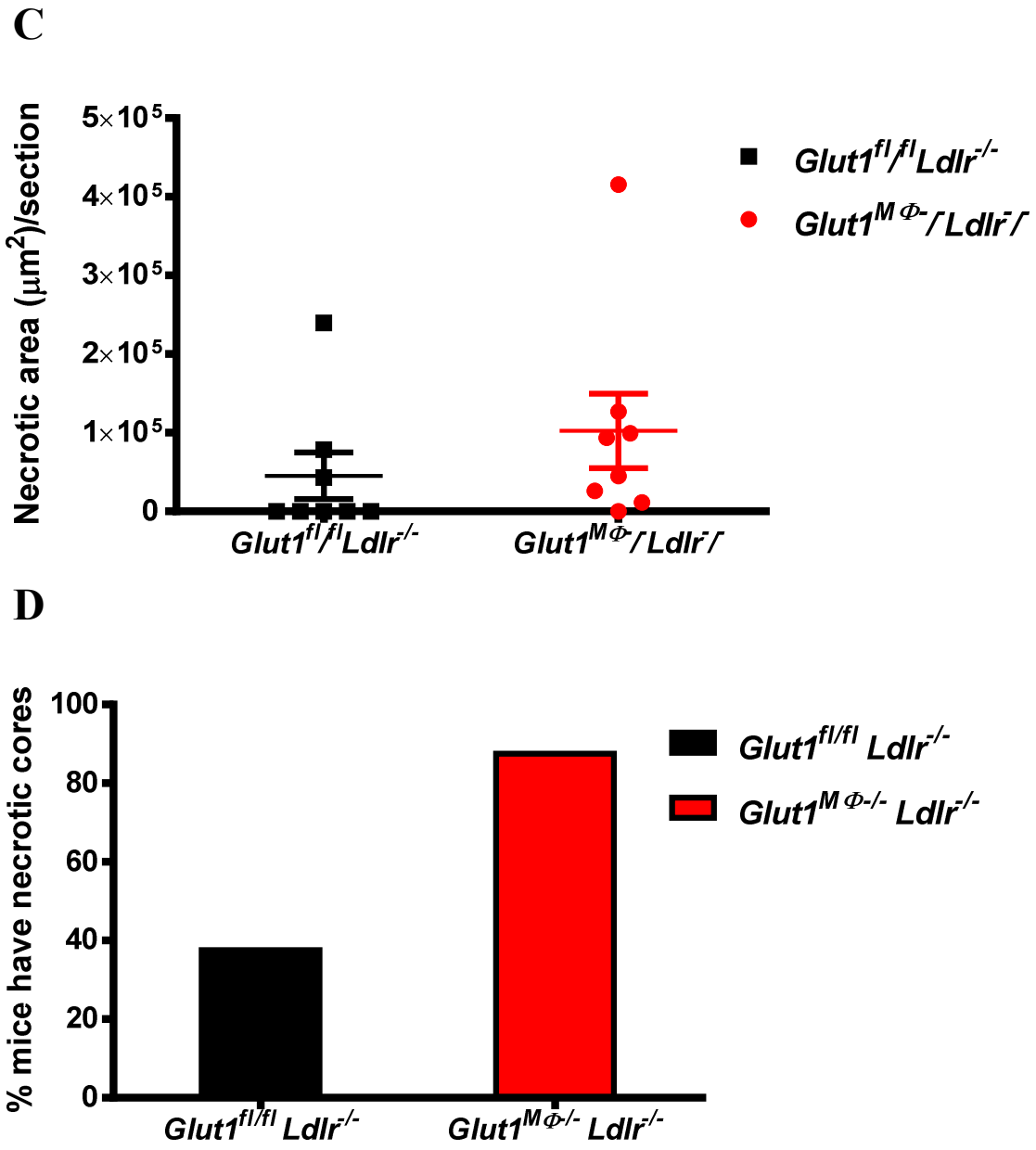

Figure 12. Increased necrotic core formation in *Ldlr*$^{-/-}$ mice reconstituted with *Glut1*$^{M\Phi-/-}$ bone marrow. (A-B) 20X representative photomicrographs of Masson's trichrome staining. Black arrow indicates representative necrotic core quantified. (C) Average necrotic area per section. Data are presented as means ± SEM, n=8. (D) Percent of *Glut1*$^{fl/fl}$ *Ldlr*$^{-/-}$ versus *Glut1*$^{M\Phi-/-}$ *Ldlr*$^{-/-}$ mice that developed necrotic core at sacrifice. n=8 per *Glut1* genotype.

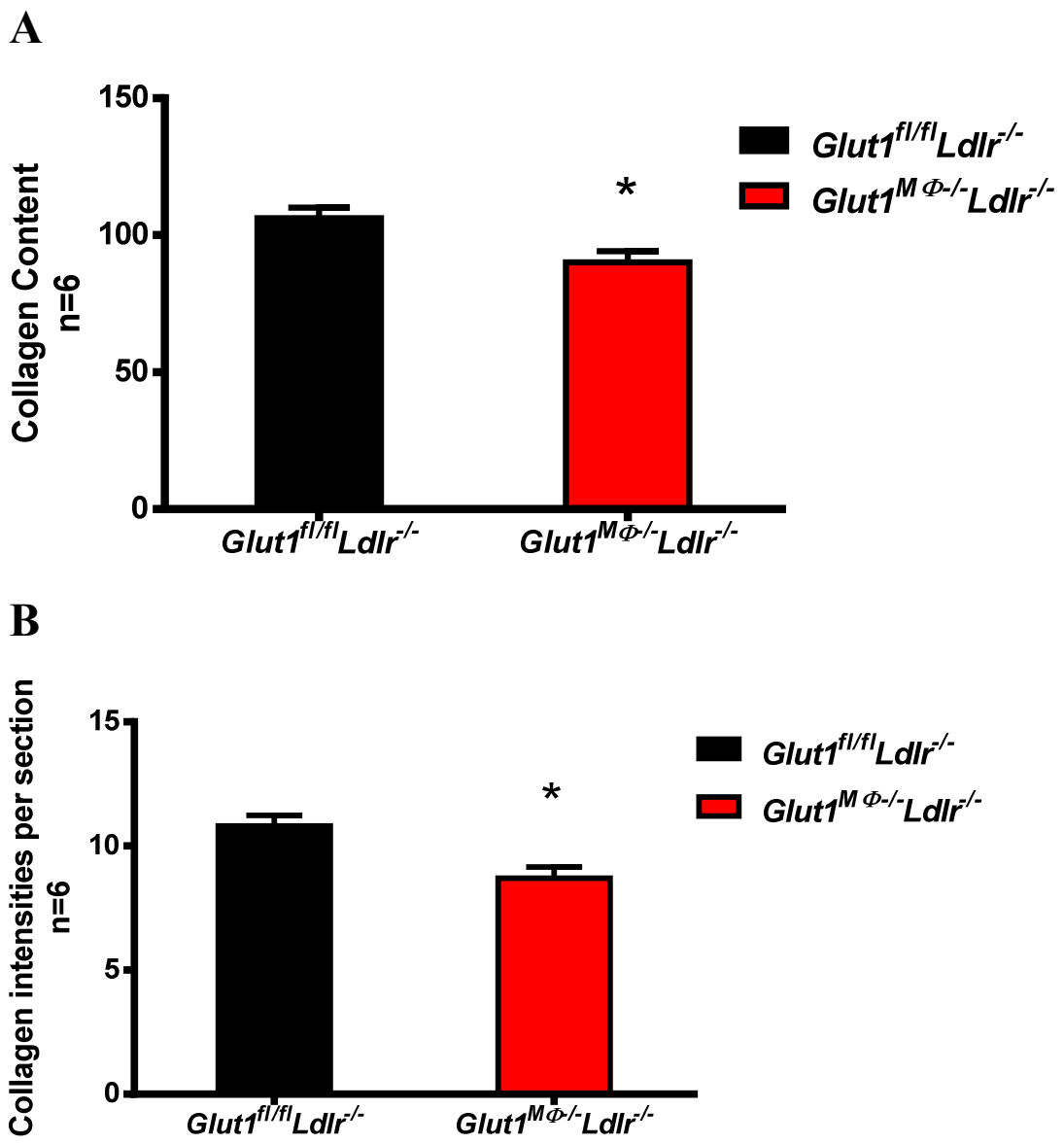

Figure 13. Lack of macrophage GLUT1 decreased collagen content in aorta sinus. Histologic analysis of collagen was performed using a color deconvolution algorithm in Aperio ScanScope software. Scores were assigned based on collagen content in regions of atherosclerotic lesions. (A) Collagen content score. (*P<0.05). (B) Calculated intensities of positive collagen staining (**P<0.01). Data are presented as means ± SEM, n = 6 per *Glut1* genotype.

A ***Glut1$^{fl/fl}$*** **peritoneal macrophages**

DAPI nucleus **Phalloidin Actin** **DIC**

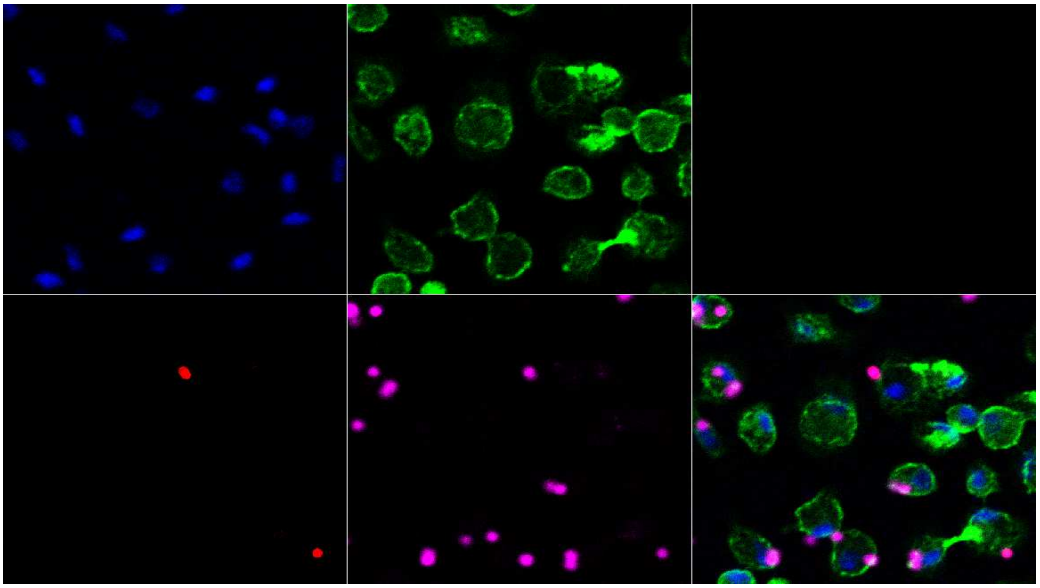

Rhodamine
Extracellular beads

Cy5
Intracellular beads

MERGE

B ***Glut1$^{M\Phi-/-}$*** **peritoneal macrophages**

DAPI nucleus **Phalloidin Actin** **DIC**

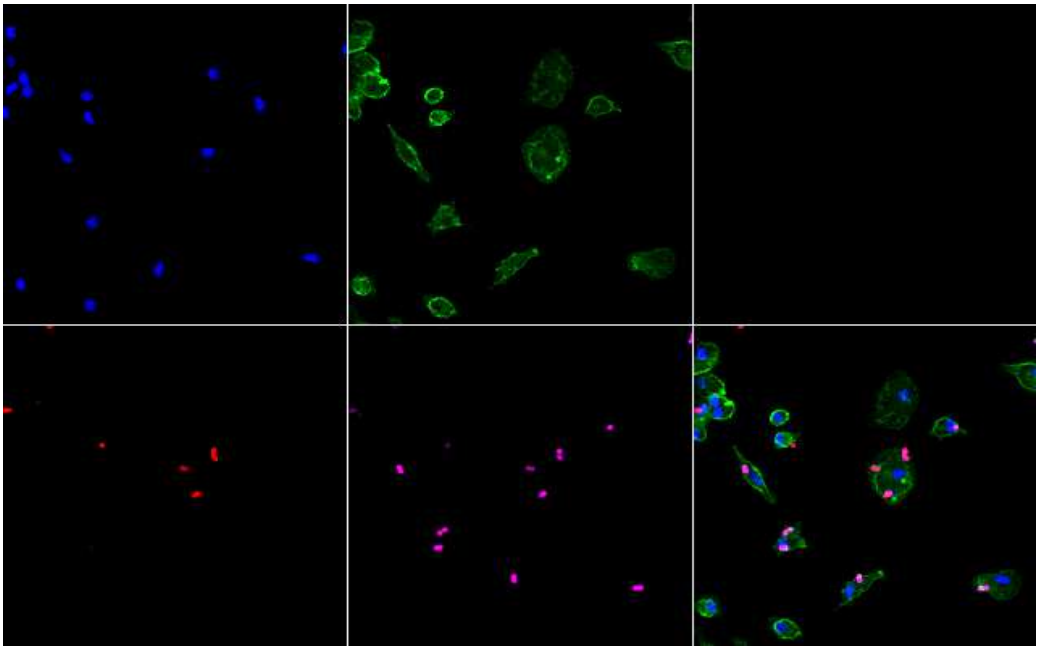

Rhodamine
Extracellular beads

Cy5
Intracellular beads

MERGE

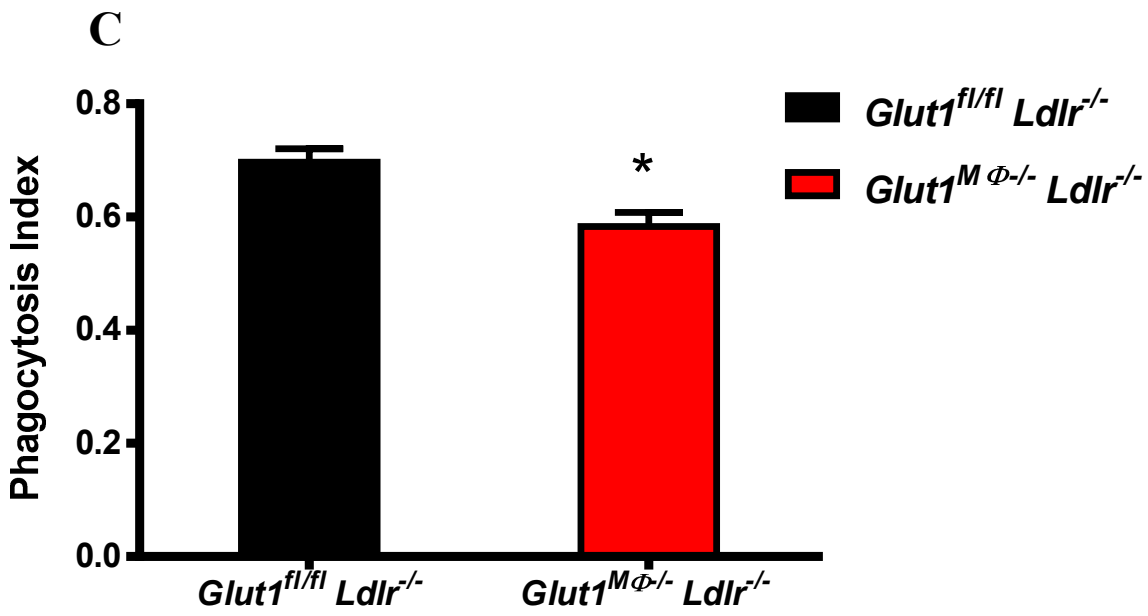

Figure 14. Lack of macrophage GLUT1 decreased phagocytosis in thioglycollate-elicited peritoneal macrophages.

(A-B) Thioglycollate-elicited peritoneal macrophages were isolated from *Glut$^{fl/fl}$* and *Glut1$^{MΦ-/-}$* mice. Macrophages were incubated with carboxylated conjugated microspheres for 20 minutes. Macrophages were stained with DAPI for nuclei (blue), phalloidin for actin (green), rhodamine for extracellular beads (red), and after permeabilization Cy5 for intracellular beads (magenta). A ZEISS LSM 700 confocal microscope was used to capture representative images (20X). (C) Phagocytosis index was calculated by numbers of microspheres taken up by macrophages (magenta)/ total microspheres in field (red and magenta). (n=1 experiment).

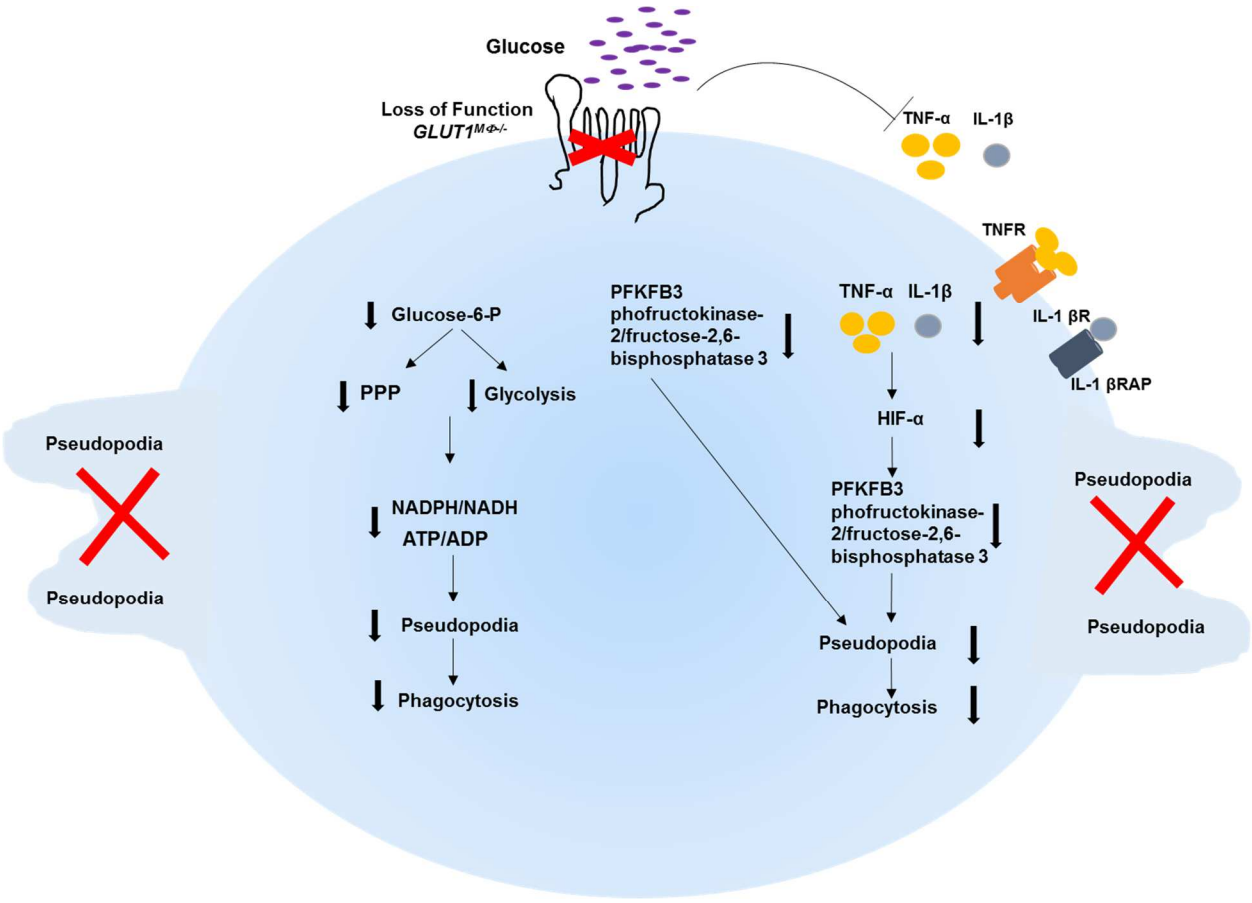

Figure 15. Working model for how decreased GLUT1-mediated glucose metabolism impairs phagocytosis. PFKFB3 maintains and supports regular cellular actin remodeling function. Reduced glucose supply decreases PFKFB3 activity, impairing macrophage phagocytic capacity. Deletion of GLUT1 reduces macrophage secretion of TNFα and IL-1β (data not shown, manuscript in preparation), which has been shown to down-regulate HIFα. HIFα increases PFKFB3 expression, therefore decreased HIFα reduces PFKFB3 expression, eventually leading to impairment of pseudopodia formation required by phagocytosis. Lastly, regular ATP/ADP and NADPH/NADP ratios maintains normal phagocytic capacity. Deletion of GLUT1 decreased glycolysis and PPP (data not shown), which potentially down regulates ATP/ADP and NADPH/NADP ratios which would impair macrophages phagocytic capacity.

CHAPTER III- DISCUSSION

Atherosclerosis is a chronic inflammatory disease and macrophages play an unparalleled role in its pathology but to date, the role of macrophage glucose metabolism on atherosclerosis remains unclear; therefore the intent of this study was to address the gap in the knowledge regarding the mechanistic link between macrophage glucose metabolism and the inflammatory response in atherogenesis by examining nutrient-responsive pathways. In 2006, Ajay Chawla demonstrated that fatty acid β-oxidation is required for alternative activation of macrophages which is involved with inflammation resolution and wound healing (Vats et al., 2006). To study the role of glucose metabolism on macrophage inflammatory response, the Makowski lab has previously published *in vitro* GLUT1 gain of function (Freemerman et al., 2014) and has obtained preliminary data using *ex vivo* GLUT1 loss of function BMDM models. These studies have demonstrated that glucose is a substrate that is required for activation of CAMs which launch the pro-inflammatory response in response to products derived from or associated with bacterial infections, such as lipopolysaccharide (LPS) and interferon gamma (IFNγ). Briefly, Freemerman et al. demonstrated that glucose transporter 1 (GLUT1) was the predominant glucose transporter on mouse BMDMs and mouse macrophage cell line RAW 264.7. Over-expression of GLUT1 on RAW cells increased their glucose uptake, glycolytic rate, and lactate production, and, more importantly, increased TNFα, IL-6, and MCP-1 gene expression (Freemerman et al., 2014). Furthermore, preliminary data showed that lack of GLUT1 significantly decreased glucose uptake and glucose oxidation, and increased fatty acid oxidation

in macrophages, indicating that lack of GLUT1 shifts macrophage substrate metabolism from glucose to fatty acid. Simultaneously, blunted glucose metabolism mediated by deletion of GLUT1 significantly reduced macrophage's capacity to mount a classical inflammatory response by inhibiting IL-1β expression, as well as components of the NLRP3 inflammasome including Caspase-3, NLRP-3, and PYCARD gene expression.

Based on our published and previous findings, we hypothesized that macrophages will have reduced inflammatory activation due to lack of GLUT1 during atherogenesis, and therefore mice carrying macrophages with deleted GLUT1 will develop reduced atherosclerosis.

Based on digital histology analysis of atherosclerotic plaque in aortic root, we demonstrated that deletion of macrophage GLUT1, originally hypothesized to mitigate atherogenesis, did not affect aorta root lesion size in *Ldlr*$^{-/-}$ mice but rather increased necrotic core formation after 12 weeks of WD exposure. Our results demonstrated that 7 out of 8 *Glut1*$^{M\Phi-/-}$ *Ldlr*$^{-/-}$ mice but only 3 out of 8 *Glut1*$^{fl/lfl}$ *Ldlr*$^{-/-}$ mice developed necrotic cores. Further, we observed that *Glut1*$^{M\Phi-/-}$ *Ldlr*$^{-/-}$ mice had significantly less collagen content in the aortic root compared to *Glut1*$^{M\Phi-/-}$ *Ldlr*$^{-/-}$ mice. Observations on systemic metabolic parameters showed that lack of macrophage GLUT1 did not affect body weight, fasting glucose, blood pressure, plasma triglyceride, or HDL cholesterol concentration. However, chimeric *Glut1*$^{M\Phi-/-}$ *Ldlr*$^{-/-}$ mice displayed increased plasma total cholesterol and LDL cholesterol. Furthermore, preliminary phagocytosis assays indicated that peritoneal macrophages collected from *Glut1*$^{M\Phi-/-}$ mice exhibited reduced phagocytic capacity compared to peritoneal macrophages collected from *Glut1*$^{fl/fl}$ mouse. The fact that *Glut1*$^{M\Phi-/-}$ macrophages showing less phagocytic capacity corroborated our histologic findings that *Glut1*$^{M\Phi-/-}$ *Ldlr*$^{-/-}$ mice displayed more and larger necrotic cores compared to *Glut1*$^{fl/fl}$ *Ldlr*$^{-/-}$ mice. Taken together, our results indicate that

macrophage GLUT1 regulates systemic lipid metabolism, and more importantly, maintenance of atherosclerotic lesion stability may be regulated by macrophage specific glucose-dependent manner. This chapter will discuss potential mechanisms leading to observed phenotypes. Additionally, this chapter will also discuss pertinent research issues, questions, and difficulties that we have confronted as well as future directions.

Effects of deletion of macrophage GLUT1 on systemic metabolic parameters

30% of adults in the United States are obese and nearly 75% are overweight. The high mortality rate tied with obesity creates a significant public health impact. Much of the mortality attributed to obesity is due to the metabolic disorders of insulin resistance, glucose intolerance, dyslipidemia, and hypertension (Odegaard & Chawla, 2011). Chronic inflammation has been shown to be a common etiologic mechanism for the collection of metabolic disorders called Metabolic Syndrome wherein macrophages play a central role in coordinating both the metabolic and inflammatory aspects. We and other have reported that GLUT1 is the primary glucose transporter in hematopoietic cells (Freemerman et al., 2014). LPS stimulation increases the rate of glycolysis and lactate production, and decreases glycogen storage in macrophages (Freemerman et al., 2014). Our first interest in the effects of deletion of macrophage's predominant glucose transporter was to study systemic metabolic parameters including body weight, body composition, fasting glucose, blood pressure, and plasma lipids. Our data showed that lack of macrophage GLUT1-mediated glucose metabolism did not affect *Ldlr*$^{-/-}$ mice body weight, body composition, and 6 hours fasted glucose after a 12 weeks of WD exposure. The results were in concert with the results from another Makowski lab's study: *Glut1*$^{fl/fl}$ and *Glut1*$^{M\Phi-/-}$ mice were either put on 10% LFD (D12450B, Research Diet, Inc., NJ) or 45% HFD (D12451, Research Diet, Inc., NJ) for 23 weeks (Freemerman et al. manuscript in prep). HFD

increased mouse body weight significantly, but there was no significant body weight difference between two genotypes indicating that macrophage GLUT1 does not play a major role in regulating mouse body weight. CAMs in adipose tissue contribute to the onset of insulin resistance through secreting pro-inflammatory cytokines such as TNF-α and IL-1β. TNF-α stimulates serine/threonine phosphorylation of insulin receptor substrate-1 (IRS-1) mediated by c-Jun N-terminal kinase (JNK) (Aguirre et al., 2002). IRS-1 serine phosphorylation disrupts regular insulin signaling pathway and has been demonstrated to lead to insulin resistance (Hotamisligil, Shargill, & Spiegelman, 1993). Genetic deletion of TNF- α or its receptor greatly attenuates deleterious effects on insulin resistance (Odegaard & Chawla, 2011; Uysal, Wiesbrock, Marino, & Hotamisligil, 1997). The Makowski lab's *ex vivo* preliminary data indicated that $Glut1^{M\Phi-/-}$ macrophages expressed significantly less TNF-α and IL-1β compared to $Glut1^{fl/fl}$ macrophages. When $Glut1^{fl/fl}$ and $Glut1^{M\Phi-/-}$ mice were made obese by a HFD, significantly more infiltrated macrophages were detected in $Glut1^{M\Phi-/-}$ epididymal white adipose tissue than in $Glut1^{fl/fl}$ mice after a 23 weeks of 45% HFD. Correspondingly, $Glut1^{M\Phi-/-}$ mice expressed increased MCP-1 in adipose tissue relative to $Glut1^{fl/fl}$ mice. Of note, while there were double the number of macrophages detected in obese $Glut1^{M\Phi-/-}$ mice, there was a lack of elevated TNF-a detected compared to $Glut1^{fl/fl}$ mice. Therefore, preliminary results indicated that $Glut1^{M\Phi-/-}$ macrophages were less inflammatory but still had the capacity, with a significantly higher tendency, to infiltrate adipose tissue compared to $Glut1^{fl/fl}$. Furthermore, flow cytometric analysis revealed that $Glut1^{M\Phi-/-}$ macrophages in obese white adipose tissue failed to polarize to CAMs and displayed greater AAMs markers compared to $Glut1^{fl/fl}$ macrophages.

We did not find any difference in blood pressure at the age of 16 weeks after a 6 week of WD exposure. Blood pressure is closely regulated by kidney, it is possible that macrophage

substrate metabolism does not play a major role in regulation of blood pressure through affecting kidney function; or 6 weeks WD may not be long enough to induce lesions which can alter blood pressure or macrophages themselves might play minor roles in blood pressure.

Glut1$^{MΦ-/-}$ *Ldlr*$^{-/-}$ mice displayed significantly higher plasma total and LDL cholesterol than *Glut1*$^{fl/fl}$ *Ldlr*$^{-/-}$ mice at the time of sacrifice. Plasma cholesterol concentration is determined by the balance of cholesterol synthesis, diet cholesterol intake and cholesterol clearance. Chronic inflammation in liver resulting from macrophage infiltration and cytokine secretion could increase liver triacylglycerol and VLDL production (Popa et al., 2007). TNF-α, IL-1β, and IL-6 increase hepatic lipogenesis through upregulating liver citrate concentration which is an allosteric activator of acetyl CoA carboxylase (ACC), the rate-limiting enzyme of the endogenous fatty acid synthesis pathway. Our preliminary data have demonstrated that GLUT1 deletion largely reduced pro-inflammatory cytokine IL-1β secretion by BMDMs *in vitro*. The observed result that *Glut1*$^{MΦ-/-}$ *Ldlr*$^{-/-}$ mice had higher plasma total and LDL cholesterol compared to *Glut1*$^{fl/fl}$ *Ldlr*$^{-/-}$ mice may seem contradictory to the preliminary data. One potential explanation for this discrepancy is that increased macrophages infiltrating into liver due to lack of GLUT1 may have caused elevated total TNF-α and IL-1β in liver which in turn increases *de novo* cholesterol synthesis (Zhao et al., 2011) Another possible interpretation is that deletion of GLUT1 tends to polarize macrophages to AAMs which requires the activation of PPARγ (Vats et al., 2006). PPARγ increases the expression of ABCA1 and ABCG1 which efflux intracellular cholesterol to HDL. HDL exchanges cholesterol with VLDL triacylglycerol mediated by cholesterol ester triglyceride transporter protein (CETP) in plasma. Taken together, we hypothesize that more *Glut1*$^{MΦ-/-}$ macrophages infiltrating into the liver to stimulate hepatic lipogenesis contributes to increased plasma cholesterol and LDL.

Effects of lack of glucose metabolism on atherosclerosis lesion

Our study sought to investigate the role of macrophage GLUT1 on the pathogenesis of atherosclerosis through a loss-of-function strategy by studying how lack of macrophage GLUT1 affects atherogenesis. Our lab has successfully manipulated hematopoietic macrophage phenotype by switching their substrate metabolism from utilizing glucose to employing fatty acid through deletion of its predominant glucose transporter 1 (GLUT1). As a result, macrophages display blunted pro-inflammatory activation due to lack of glucose metabolism. Inflammation is the major pathological process of atherosclerosis development. We originally hypothesized that deletion of GLUT1 on macrophages would decrease atherogenesis. However, after a 12 week WD exposure, we did not observe significant differences in lesion size in aorta sinus between *GLUT1*$^{fl/fl}$ *Ldlr*$^{-/-}$ and *GLUT1*$^{M\Phi-/-}$ *Ldlr*$^{-/-}$ mice. Nishizawa et al. recently published an investigation of how over-expressed macrophage GLUT1 altered atherogenesis. They demonstrated that overexpression of macrophage GLUT1 did not increase lesion size (Nishizawa et al., 2014). Both studies intended to investigate the role of macrophage GLUT1 but utilizing opposite strategies: we utilized loss-of-function strategy by deletion of macrophage GLUT1 and they used gain-of-function method by over-expression macrophage GLUT1. Our result is consistent with Nishizawa's result that macrophage GLUT1 mediated glucose metabolism does not affect atherosclerosis lesion size per se (Ma et al., 2012; Nishizawa et al., 2014).

Effects of lack of glucose metabolism on necrotic cores

The majority of cardiovascular clinical events result from consequences of lesion rupture instead of lesion-caused blood vessel stenosis. The unstable atherosclerotic plaque is characterized by large necrotic core appearance and thinning of the fibrotic cap. Glucose is a

critical energy source for maintaining proper immune cell function. The glycolysis pathway is essential in triggering the respiratory burst and facilitating actin cytoskeleton rearrangement, which is associated with macrophage phagocytic capacity and therefore could potentially affect lesion necrotic core formation. We observed 7 out 8 *Glut1*$^{M\Phi-/-}$ *Ldlr*$^{-/-}$ mice developed necrotic cores but only 3 out 8 *Glut1*$^{fl/fl}$ *Ldlr*$^{-/-}$ mice formed necrotic area after a 12 weeks of WD exposure. The result did not reach statistical significance due to relatively small sample size. 16 mice from each genetic group were used for our study, but hearts from 8 mice from each genotype were used for studying lesion size. Hearts used for studying lesion size were embedded in Optimal Cutting Temperature (OCT) and used for ORO staining, which is a method to study lipid accumulation. Unfortunately, ORO can't be used to study lesion morphology and structure, therefore only n=8 mice from each group were used for quantifying lesion morphology. In future studies, we will conduct more experiments to increase our sample size or develop an alternative protocol such as only staining heart sections with Masson's trichrome.

Macrophage phagocytosis is a process that involves cooperative interaction among receptors, exogenous substances, and actin filaments. Rearrangement of the actin cytoskeleton is essential to macrophage function and is considered to be an energy draining process (Everett, Barghouthi, & Speert, 1996; Venter et al., 2014). The dynamics of actin cytoskeleton remodeling is determined by ATP/ADP ratio, NAD (P)/NAD (P)H ratio, and intracellular pH. Glucose participates in three major metabolic pathways including glycolysis, glycogen synthesis, and Pentose Phosphate Pathway (PPP). PPP is the cell's major source for riboses and NADPHs, which, respectively, are building blocks for DNA and intracellular reducing agents. Freemerman et al. demonstrated that over-expression of GLUT1 in RAW246.7 cells increased PPP metabolites. Conversely lack of GLUT1 in BMDMs decreased PPP metabolites (data not

shown), indicating that overexpression or deletion macrophage's predominant glucose transporter GLUT1 can alter cells NADP/NADPH ratio, therefore could be one potential mechanism to change macrophage's phagocytic capacity.

Several glycolytic enzymes are associated with the actin cytoskeleton and with actin-dependent cellular structures, such as pseudopodia, membrane ruffles, and lamellipodia (Venter et al., 2014). Therefore, glucose metabolism and actin-based cell dynamics are tied together. LPS stimulates the macrophage to become pro-inflammatory through classically activated pathway which induces a shift in macrophage redox potential, accompanied by increased flux through glycolysis as well as the PPP for NADPH production (Venter et al., 2014). Murine peritoneal macrophages express GLUT1 which mediates the transport of 2-deoxyglucose, glucose, and mannose into the macrophage. Phagocytic capacity of peritoneal macrophages is inhibited by a low concentration of non-metabolizable 2-deoxyglucose indicating that an intracellular metabolite of glucose may trigger phagocytosis (Everett et al., 1996). Nishizawa et al. showed that in BMDMs 6-phosphofructo-2-kinase/fructose-2,6-biphosphatase 3 (PFKFB3) expression along with hexokinase-3 (HK-3) significantly increased upon LPS treatment but decreased with GLUT1 knocked down by siRNA.(Nishizawa et al., 2014). Similar to macrophages, endothelial cells are highly glycolytic and PFKFB3 controls the formation of filopodia/lamellipodia, which are actin projections on the leading edge of cell; PFKFB3 silencing impairs lamellipodia formation (De Bock et al., 2013). **Taken together, we hypothesize that *Glut1*$^{M\Phi-/-}$ macrophages have reduced PFKFB3 activity leading to defective actin cytoskeleton remodeling and efferocytosis; apoptotic cell debris in atherosclerotic lesions are not effectively cleared by *Glut1*$^{M\Phi-/-}$ macrophages therefore more and larger necrotic cores are evident.**

Interestingly, we found differences in necrotic cores, but Nishizawa's study did not observe difference in necrotic areas. One possible interpretation for this disparity is that manipulating macrophage's metabolism into more glycolytic through overexpression of GLUT1 increases PFKFB3 expression, which either maintains or increases macrophage's phagocytic capacity. Deletion of macrophage GLUT1 inhibits the glycolysis pathway and therefore PFKFB3 expression is suppressed which impairs the cell's phagocytic capacity (Figure 15). Another explanation for the observed disparity is that in our model chimeric *Ldlr*$^{-/-}$ mice were on high cholesterol atherogenic diet for 12 weeks but chimeric *Ldlr*$^{-/-}$ mice in Nishizawa's study were on 10% low fat diet for 22 weeks. In summary, by utilizing either gain-of-function or loss-of-function strategy Nishizawa et al and we observed different results of atherosclerotic necrotic cores which may result from different PFKFB3 enzyme activities or diet feeding paradigms.

Consideration of Study Design

In order to specifically delete GLUT1 in macrophages, we crossed LysM-Cre mouse with *Glut1*$^{fl/fl}$ mice. Cre recombinase was inserted after the promoter for the lysozyme 2 gene. Knocking in Cre recombinase in the location of Lysozyme 2 gene abolishes Lysozyme 2 expression but turns on Cre recombinase expression under the control of the endogenous Lysozyme2 promoter/enhance elements. Lysozyme 2 is expressed in the myeloid cell lineage including monocytes, mature macrophages, and granulocytes. Two LoxP sites were inserted respectively at intron 2 and intron 9 of the mouse *Glut1* gene (Young et al., 2011). When we crossed *LysM-Cre* mice with *Glut1*$^{fl/fl}$ mice, *Glut1* was successfully deleted in macrophages (manuscript in preparation). Since Lysozyme 2 is expressed in all cells from myeloid origin, neutrophil *Glut1* is simultaneously deleted, we will investigate the role of lack of neutrophil GLUT1 on atherosclerosis in the future.

We employed BMT model to study the role of macrophage GLUT1 on the pathogenesis of atherosclerosis. BMT model has been extensively used in studying cells from hematopoietic origins. A lethal dose of irradiation ablates the hematopoietic system, but transplanting viable hematopoietic stem progenitor cells into irradiated animals that will salvage their hematopoietic systems by reconstitution. By day 21 after BMT, peripheral hematopoietic reconstitution of all cell lineage numbers may reach normal levels but many of the innate cellular effectors are yet not fully functional. If the donor hematopoietic stem cells fail to engraft, recipients eventually will succumb to infection secondary to bone marrow aplasia, anemia, or thrombocytopenia (Duran-Struuck & Dysko, 2009). In our experiments, we let the recipient mice reconstitute for 4 weeks before performing other experiment procedures. *Ldlr*$^{-/-}$ mice develop small fatty streaks on the aorta after 4 weeks on WD (Aslanian, Chapman, & Charo, 2005) and exhibit endothelial disruption and an accumulation of macrophage and foam cells at the site of atherosclerotic plaques after 12 weeks on a high cholesterol diet (Mehta et al., 2007). We chose our study endpoint at the age of 22 weeks which is after 12 weeks on WD. A glycolysis-driven metabolic program prompts macrophages to trigger rapid and vigorous responses toward infection, therefore it is possible that we might miss the dynamics of *Glut1*$^{M\Phi-/-}$ driven atherosclerosis development after 12 weeks WD exposure. Given the unique role of glucose metabolism on macrophages, it might be helpful to conduct experiments to study different lengths of WD exposure.

Future Studies and Implications of Our Findings

We observed that 7 out of 8 *Glut1*$^{M\Phi-/-}$ *Ldlr*$^{-/-}$ mice developed necrotic cores but only 3 out 8 *Glut1*$^{fl/fl}$ *Ldlr*$^{-/-}$ mice formed necrotic cores after 12 weeks WD exposure. We had total n=16 mice in each genotype, but only used 8 mice from individual genotype for analyzing lesion

morphology. We observed a more than 50% increase in necrotic area (μm^2) in *Glut1*$^{M\Phi-/-}$ *Ldlr*$^{-/-}$ relative to *Glut1*$^{fl/fl}$ *Ldlr*$^{-/-}$ mice, and 87.5% of *Glut1*$^{M\Phi-/-}$ *Ldlr*$^{-/-}$ mice but only 37.5% of *Glut1*$^{fl/fl}$ *Ldlr*$^{-/-}$ mice developed necrotic cores. However, limited by the number of animals, necrotic core differences between the two study groups did not reach statistical significance. First and foremost, we need to increase our study power by increasing our sample size in order to detect significant differences in necrotic area. Next, we observed an increase in plasma total cholesterol and LDL cholesterol in *Glut1*$^{M\Phi-/-}$ *Ldlr*$^{-/-}$ mice than *Glut1*$^{fl/fl}$ *Ldlr*$^{-/-}$ mice. Increased plasma total cholesterol and LDL cholesterol are secondary to either increased VLDL export from liver or decreased cholesterol clearance. We harvested liver when we sacrificed mice, therefore measuring liver triacylglycerol and cholesterol concentrations could generate evidence whether there is difference in the lipid accumulation in liver. Examining liver macrophage infiltration and subtypes would be informative as to whether there is increased macrophage infiltration in *GLUT1*$^{M\Phi-/-}$ *Ldlr*$^{-/-}$ livers.

Our pilot phagocytosis assay indicated that macrophages without GLUT1 have decreased phagocytic capacities. We need to repeat this experiment to confirm our findings. Since the phagocytosis assay was conducted using mouse IgG opsonized microspheres, efferocytosis assays wherein macrophages engulf apoptotic cell debris need to be conducted in order to recapitulate what happen *in vivo* more closely.

In summary, this study provides evidence for the first time that macrophage GLUT1 dependent glucose metabolism plays a critical role in maintaining atherosclerotic lesion stability. The results shed light on the potential mechanistic link between macrophage GLUT1 mediated glucose metabolism and pathogenesis of atherosclerotic. Through “metabolically reprograming” the inflammatory potential of macrophages via GLUT1 mediated pathways, we have

demonstrated that lack of macrophage GLUT1 protected mice from HFD-induced obesity. Macrophages are an extremely heterogeneous population of cells with the capacity for metabolic flexibility with important implications for both systemic and local responses. Therefore, our particular model warrants further investigation of the temporal and spatial control of chronic inflammatory disease with macrophage GLUT1 mediated glucose metabolism.

REFERENCES

Aguirre, V., Werner, E. D., Giraud, J., Lee, Y. H., Shoelson, S. E., & White, M. F. (2002). Phosphorylation of Ser307 in insulin receptor substrate-1 blocks interactions with the insulin receptor and inhibits insulin action. *The Journal of Biological Chemistry, 277*(2), 1531-1537. doi:10.1074/jbc.M101521200 [doi]

Alexander, R. W. (1995). Theodore cooper memorial lecture. hypertension and the pathogenesis of atherosclerosis. oxidative stress and the mediation of arterial inflammatory response: A new perspective. *Hypertension, 25*(2), 155-161.

Altman, R. (2003). Risk factors in coronary atherosclerosis athero-inflammation: The meeting point. *Thrombosis Journal, 1*(1), 4. doi:10.1186/1477-9560-1-4 [doi]

Aslanian, A. M., Chapman, H. A., & Charo, I. F. (2005). Transient role for CD1d-restricted natural killer T cells in the formation of atherosclerotic lesions. *Arteriosclerosis, Thrombosis, and Vascular Biology, 25*(3), 628-632. doi:01.ATV.0000153046.59370.13 [pii]

Becker, L., Gharib, S. A., Irwin, A. D., Wijsman, E., Vaisar, T., Oram, J. F., & Heinecke, J. W. (2010). A macrophage sterol-responsive network linked to atherogenesis. *Cell Metabolism, 11*(2), 125-135. doi:10.1016/j.cmet.2010.01.003 [doi]

Bjorkbacka, H., Kunjathoor, V. V., Moore, K. J., Koehn, S., Ordija, C. M., Lee, M. A., . . . Freeman, M. W. (2004). Reduced atherosclerosis in MyD88-null mice links elevated serum cholesterol levels to activation of innate immunity signaling pathways. *Nature Medicine, 10*(4), 416-421. doi:10.1038/nm1008 [doi]

Boullier, A., Bird, D. A., Chang, M. K., Dennis, E. A., Friedman, P., Gillotre-Taylor, K., . . . Witztum, J. L. (2001). Scavenger receptors, oxidized LDL, and atherosclerosis. *Annals of the New York Academy of Sciences, 947*, 214-22; discussion 222-3.

Boyle, J. J., Weissberg, P. L., & Bennett, M. R. (2003). Tumor necrosis factor-alpha promotes macrophage-induced vascular smooth muscle cell apoptosis by direct and autocrine mechanisms. *Arteriosclerosis, Thrombosis, and Vascular Biology, 23*(9), 1553-1558. doi:10.1161/01.ATV.0000086961.44581.B7 [doi]

Chade, A. R., Lerman, A., & Lerman, L. O. (2005). Kidney in early atherosclerosis. *Hypertension, 45*(6), 1042-1049. doi:01.HYP.0000167121.14254.a0 [pii]

Chawla, A., Nguyen, K. D., & Goh, Y. P. (2011). Macrophage-mediated inflammation in metabolic disease. *Nature Reviews.Immunology, 11*(11), 738-749. doi:10.1038/nri3071 [doi]

Chinetti-Gbaguidi, G., Colin, S., & Staels, B. (2015). Macrophage subsets in atherosclerosis. *Nature Reviews.Cardiology, 12*(1), 10-17. doi:10.1038/nrcardio.2014.173 [doi]

Chinetti-Gbaguidi, G., & Staels, B. (2011). Macrophage polarization in metabolic disorders: Functions and regulation. *Current Opinion in Lipidology, 22*(5), 365-372. doi:10.1097/MOL.0b013e32834a77b4 [doi]

Coppolino, M. G., Dierckman, R., Loijens, J., Collins, R. F., Pouladi, M., Jongstra-Bilen, J., . . . Grinstein, S. (2002). Inhibition of phosphatidylinositol-4-phosphate 5-kinase ialpha impairs localized actin remodeling and suppresses phagocytosis. *The Journal of Biological Chemistry, 277*(46), 43849-43857. doi:10.1074/jbc.M209046200 [doi]

De Bock, K., Georgiadou, M., Schoors, S., Kuchnio, A., Wong, B. W., Cantelmo, A. R., . . . Carmeliet, P. (2013). Role of PFKFB3-driven glycolysis in vessel sprouting. *Cell, 154*(3), 651-663. doi:10.1016/j.cell.2013.06.037 [doi]

Di Luozzo, G. (2012). http://www.aortarepair.com/anatomy.html.

Dickhout, J. G., Basseri, S., & Austin, R. C. (2008). Macrophage function and its impact on atherosclerotic lesion composition, progression, and stability: The good, the bad, and the ugly. *Arteriosclerosis, Thrombosis, and Vascular Biology, 28*(8), 1413-1415. doi:10.1161/ATVBAHA.108.169144 [doi]

Duewell, P., Kono, H., Rayner, K. J., Sirois, C. M., Vladimer, G., Bauernfeind, F. G., . . . Latz, E. (2010). NLRP3 inflammasomes are required for atherogenesis and activated by cholesterol crystals. *Nature, 464*(7293), 1357-1361. doi:10.1038/nature08938 [doi]

Duran-Struuck, R., & Dysko, R. C. (2009). Principles of bone marrow transplantation (BMT): Providing optimal veterinary and husbandry care to irradiated mice in BMT studies. *Journal of the American Association for Laboratory Animal Science : JAALAS, 48*(1), 11-22.

Erbay, E., Babaev, V. R., Mayers, J. R., Makowski, L., Charles, K. N., Snitow, M. E., . . . Hotamisligil, G. S. (2009). Reducing endoplasmic reticulum stress through a macrophage lipid chaperone alleviates atherosclerosis. *Nature Medicine, 15*(12), 1383-1391. doi:10.1038/nm.2067 [doi]

Everett, K. D., Barghouthi, S., & Speert, D. P. (1996). In vitro culture of murine peritoneal and alveolar macrophages modulates phagocytosis of pseudomonas aeruginosa and glucose transport. *Journal of Leukocyte Biology, 59*(4), 539-544.

Flannagan, R. S., Jaumouille, V., & Grinstein, S. (2012). The cell biology of phagocytosis. *Annual Review of Pathology, 7*, 61-98. doi:10.1146/annurev-pathol-011811-132445 [doi]

Freemerman, A. J., Johnson, A. R., Sacks, G. N., Milner, J. J., Kirk, E. L., Troester, M. A., . . . Makowski, L. (2014). Metabolic reprogramming of macrophages: Glucose transporter 1 (GLUT1)-mediated glucose metabolism drives a proinflammatory phenotype. *The Journal of Biological Chemistry, 289*(11), 7884-7896. doi:10.1074/jbc.M113.522037 [doi]

Frostegard, J. (2013). Immunity, atherosclerosis and cardiovascular disease. *BMC Medicine, 11*, 117-7015-11-117. doi:10.1186/1741-7015-11-117 [doi]

Fruchart, J. C., Nierman, M. C., Stroes, E. S., Kastelein, J. J., & Duriez, P. (2004). New risk factors for atherosclerosis and patient risk assessment. *Circulation, 109*(23 Suppl 1), III15-9. doi:10.1161/01.CIR.0000131513.33892.5b [doi]

Geissmann, F., Jung, S., & Littman, D. R. (2003). Blood monocytes consist of two principal subsets with distinct migratory properties. *Immunity, 19*(1), 71-82. doi:S1074761303001742 [pii]

Getz, G. S., & Reardon, C. A. (2012). Animal models of atherosclerosis. *Arteriosclerosis, Thrombosis, and Vascular Biology, 32*(5), 1104-1115. doi:10.1161/ATVBAHA.111.237693 [doi]

Grundy, S. M. (2002). Obesity, metabolic syndrome, and coronary atherosclerosis. *Circulation, 105*(23), 2696-2698.

Hess, K., Marx, N., & Lehrke Michael. (2012). Cardiovascular disease and diabetes: The vulnerable patient., B4-B13. doi:http://dx.doi.org/10.1093/eurheartj/sus002

Hopkins, P. N. (2013). Molecular biology of atherosclerosis. *Physiological Reviews, 93*(3), 1317-1542. doi:10.1152/physrev.00004.2012 [doi]

Horton, J. D., Goldstein, J. L., & Brown, M. S. (2002). SREBPs: Activators of the complete program of cholesterol and fatty acid synthesis in the liver. *The Journal of Clinical Investigation, 109*(9), 1125-1131. doi:10.1172/JCI15593 [doi]

Hotamisligil, G. S., Shargill, N. S., & Spiegelman, B. M. (1993). Adipose expression of tumor necrosis factor-alpha: Direct role in obesity-linked insulin resistance. *Science (New York, N.Y.), 259*(5091), 87-91.

Johnson, A. R., Milner, J. J., & Makowski, L. (2012). The inflammation highway: Metabolism accelerates inflammatory traffic in obesity. *Immunological Reviews, 249*(1), 218-238. doi:10.1111/j.1600-065X.2012.01151.x [doi]

Kolovou, G., Anagnostopoulou, K., Mikhailidis, D. P., & Cokkinos, D. V. (2008). Apolipoprotein E knockout models. *Current Pharmaceutical Design, 14*(4), 338-351.

Leitinger, N., & Schulman, I. G. (2013). Phenotypic polarization of macrophages in atherosclerosis. *Arteriosclerosis, Thrombosis, and Vascular Biology, 33*(6), 1120-1126. doi:10.1161/ATVBAHA.112.300173 [doi]

Lumeng, C. N., Bodzin, J. L., & Saltiel, A. R. (2007). Obesity induces a phenotypic switch in adipose tissue macrophage polarization. *The Journal of Clinical Investigation, 117*(1), 175-184. doi:10.1172/JCI29881 [doi]

Lusis, A. J. (2000). Atherosclerosis. *Nature, 407*(6801), 233-241. doi:10.1038/35025203 [doi]

Ma, Y., Wang, W., Zhang, J., Lu, Y., Wu, W., Yan, H., & Wang, Y. (2012). Hyperlipidemia and atherosclerotic lesion development in ldlr-deficient mice on a long-term high-fat diet. *PloS One, 7*(4), e35835. doi:10.1371/journal.pone.0035835 [doi]

Makowski, L., Boord, J. B., Maeda, K., Babaev, V. R., Uysal, K. T., Morgan, M. A., . . . Linton, M. F. (2001a). Lack of macrophage fatty-acid-binding protein aP2 protects mice deficient in apolipoprotein E against atherosclerosis. *Nature Medicine, 7*(6), 699-705. doi:10.1038/89076 [doi]

Makowski, L., Boord, J. B., Maeda, K., Babaev, V. R., Uysal, K. T., Morgan, M. A., . . . Linton, M. F. (2001b). Lack of macrophage fatty-acid-binding protein aP2 protects mice deficient in apolipoprotein E against atherosclerosis. *Nature Medicine, 7*(6), 699-705. doi:10.1038/89076 [doi]

Makowski, L., Brittingham, K. C., Reynolds, J. M., Suttles, J., & Hotamisligil, G. S. (2005). The fatty acid-binding protein, aP2, coordinates macrophage cholesterol trafficking and inflammatory activity. macrophage expression of aP2 impacts peroxisome proliferator-activated receptor gamma and IkappaB kinase activities. *The Journal of Biological Chemistry, 280*(13), 12888-12895. doi:M413788200 [pii]

Mehta, J. L., Sanada, N., Hu, C. P., Chen, J., Dandapat, A., Sugawara, F., . . . Sawamura, T. (2007). Deletion of LOX-1 reduces atherogenesis in LDLR knockout mice fed high cholesterol diet. *Circulation Research, 100*(11), 1634-1642. doi:CIRCRESAHA.107.149724 [pii]

Moore, K. J., Sheedy, F. J., & Fisher, E. A. (2013). Macrophages in atherosclerosis: A dynamic balance. *Nature Reviews.Immunology, 13*(10), 709-721. doi:10.1038/nri3520 [doi]

Moore, K. J., & Tabas, I. (2011). Macrophages in the pathogenesis of atherosclerosis. *Cell, 145*(3), 341-355. doi:10.1016/j.cell.2011.04.005 [doi]

Nishizawa, T., Kanter, J. E., Kramer, F., Barnhart, S., Shen, X., Vivekanandan-Giri, A., . . . Bornfeldt, K. E. (2014). Testing the role of myeloid cell glucose flux in inflammation and atherosclerosis. *Cell Reports, 7*(2), 356-365. doi:10.1016/j.celrep.2014.03.028 [doi]

Odegaard, J. I., & Chawla, A. (2011). Alternative macrophage activation and metabolism. *Annual Review of Pathology, 6*, 275-297. doi:10.1146/annurev-pathol-011110-130138 [doi]

Odegaard, J. I., Ricardo-Gonzalez, R. R., Goforth, M. H., Morel, C. R., Subramanian, V., Mukundan, L., . . . Chawla, A. (2007a). Macrophage-specific PPARgamma controls alternative activation and improves insulin resistance. *Nature, 447*(7148), 1116-1120. doi:nature05894 [pii]

Odegaard, J. I., Ricardo-Gonzalez, R. R., Goforth, M. H., Morel, C. R., Subramanian, V., Mukundan, L., . . . Chawla, A. (2007b). Macrophage-specific PPARgamma controls alternative activation and improves insulin resistance. *Nature, 447*(7148), 1116-1120. doi:nature05894 [pii]

Peled, M., & Fisher, E. A. (2014). Dynamic aspects of macrophage polarization during atherosclerosis progression and regression. *Frontiers in Immunology, 5*, 579. doi:10.3389/fimmu.2014.00579 [doi]

Popa, C., Netea, M. G., van Riel, P. L., van der Meer, J. W., & Stalenhoef, A. F. (2007). The role of TNF-alpha in chronic inflammatory conditions, intermediary metabolism, and cardiovascular risk. *Journal of Lipid Research, 48*(4), 751-762. doi:R600021-JLR200 [pii]

Randolph, G. J. (2014). Mechanisms that regulate macrophage burden in atherosclerosis. *Circulation Research, 114*(11), 1757-1771. doi:10.1161/CIRCRESAHA.114.301174 [doi]

Rotllan, N., Chamorro-Jorganes, A., Araldi, E., Wanschel, A. C., Aryal, B., Aranda, J. F., . . . Fernandez-Hernando, C. (2015). Hematopoietic Akt2 deficiency attenuates the progression of atherosclerosis. *FASEB Journal : Official Publication of the Federation of American Societies for Experimental Biology, 29*(2), 597-610. doi:10.1096/fj.14-262097 [doi]

Schrijvers, D. M., De Meyer, G. R., Herman, A. G., & Martinet, W. (2007). Phagocytosis in atherosclerosis: Molecular mechanisms and implications for plaque progression and stability. *Cardiovascular Research, 73*(3), 470-480. doi:S0008-6363(06)00404-4 [pii]

Seimon, T., & Tabas, I. (2009). Mechanisms and consequences of macrophage apoptosis in atherosclerosis. *Journal of Lipid Research, 50 Suppl*, S382-7. doi:10.1194/jlr.R800032-JLR200 [doi]

Stary, H. C., Chandler, A. B., Dinsmore, R. E., Fuster, V., Glagov, S., Insull, W.,Jr, . . . Wissler, R. W. (1995). A definition of advanced types of atherosclerotic lesions and a histological classification of atherosclerosis. A report from the committee on vascular lesions of the council on arteriosclerosis, american heart association. *Arteriosclerosis, Thrombosis, and Vascular Biology, 15*(9), 1512-1531.

Steinberg, D. (2013). In celebration of the 100th anniversary of the lipid hypothesis of atherosclerosis. *Journal of Lipid Research, 54*(11), 2946-2949. doi:10.1194/jlr.R043414 [doi]

Subramanian, M., Thorp, E., & Tabas, I. (2015). Identification of a non-growth factor role for GM-CSF in advanced atherosclerosis: Promotion of macrophage apoptosis and plaque necrosis through IL-23 signaling. *Circulation Research, 116*(2), e13-24. doi:10.1161/CIRCRESAHA.116.304794 [doi]

Sundaram, S., Freemerman, A. J., Johnson, A. R., Milner, J. J., McNaughton, K. K., Galanko, J. A., . . . Makowski, L. (2013). Role of HGF in obesity-associated tumorigenesis: C3(1)-TAg

mice as a model for human basal-like breast cancer. *Breast Cancer Research and Treatment, 142*(3), 489-503. doi:10.1007/s10549-013-2741-5 [doi]

Swirski, F. K., Libby, P., Aikawa, E., Alcaide, P., Luscinskas, F. W., Weissleder, R., & Pittet, M. J. (2007). Ly-6Chi monocytes dominate hypercholesterolemia-associated monocytosis and give rise to macrophages in atheromata. *The Journal of Clinical Investigation, 117*(1), 195-205. doi:10.1172/JCI29950 [doi]

Tabas, I., Williams, K. J., & Boren, J. (2007). Subendothelial lipoprotein retention as the initiating process in atherosclerosis: Update and therapeutic implications. *Circulation, 116*(16), 1832-1844. doi:116/16/1832 [pii]

Uysal, K. T., Wiesbrock, S. M., Marino, M. W., & Hotamisligil, G. S. (1997). Protection from obesity-induced insulin resistance in mice lacking TNF-alpha function. *Nature, 389*(6651), 610-614. doi:10.1038/39335 [doi]

Van Vre, E. A., Ait-Oufella, H., Tedgui, A., & Mallat, Z. (2012). Apoptotic cell death and efferocytosis in atherosclerosis. *Arteriosclerosis, Thrombosis, and Vascular Biology, 32*(4), 887-893. doi:10.1161/ATVBAHA.111.224873 [doi]

Vats, D., Mukundan, L., Odegaard, J. I., Zhang, L., Smith, K. L., Morel, C. R., . . . Chawla, A. (2006). Oxidative metabolism and PGC-1beta attenuate macrophage-mediated inflammation. *Cell Metabolism, 4*(1), 13-24. doi:S1550-4131(06)00202-6 [pii]

Venter, G., Oerlemans, F. T., Wijers, M., Willemse, M., Fransen, J. A., & Wieringa, B. (2014). Glucose controls morphodynamics of LPS-stimulated macrophages. *PloS One, 9*(5), e96786. doi:10.1371/journal.pone.0096786 [doi]

Virmani, R., Burke, A. P., Farb, A., & Kolodgie, F. D. (2002). Pathology of the unstable plaque. *Progress in Cardiovascular Diseases, 44*(5), 349-356. doi:S0033062002500116 [pii]

Wassink, A. M., Van Der Graaf, Y., Soedamah-Muthu, S. S., Spiering, W., Visseren, F. L., & Smart Study Group. (2008). Metabolic syndrome and incidence of type 2 diabetes in patients with manifest vascular disease. *Diabetes & Vascular Disease Research : Official Journal of the International Society of Diabetes and Vascular Disease, 5*(2), 114-122. doi:10.3132/dvdr.2008.019 [doi]

Young, C. D., Lewis, A. S., Rudolph, M. C., Ruehle, M. D., Jackman, M. R., Yun, U. J., . . . Anderson, S. M. (2011). Modulation of glucose transporter 1 (GLUT1) expression levels alters mouse mammary tumor cell growth in vitro and in vivo. *PloS One, 6*(8), e23205. doi:10.1371/journal.pone.0023205 [doi]

Zhang, X., Goncalves, R., & Mosser, D. M. (2008). The isolation and characterization of murine macrophages. *Current Protocols in Immunology / Edited by John E.Coligan ...[Et Al.], Chapter 14*, Unit 14.1. doi:10.1002/0471142735.im1401s83 [doi]

Zhao, L., Chen, Y., Tang, R., Chen, Y., Li, Q., Gong, J., . . . Ruan, X. Z. (2011). Inflammatory stress exacerbates hepatic cholesterol accumulation via increasing cholesterol uptake and de novo synthesis. *Journal of Gastroenterology and Hepatology, 26*(5), 875-883. doi:10.1111/j.1440-1746.2010.06560.x [doi]

Zhou, R. H., Vendrov, A. E., Tchivilev, I., Niu, X. L., Molnar, K. C., Rojas, M., . . . Runge, M. S. (2012). Mitochondrial oxidative stress in aortic stiffening with age: The role of smooth muscle cell function. *Arteriosclerosis, Thrombosis, and Vascular Biology, 32*(3), 745-755. doi:10.1161/ATVBAHA.111.243121 [doi]